④

TECHNICAL REPORT BRL-TR-3072

BRL

AD-A218 556

A COMPARISON BETWEEN EXPERIMENT
AND SIMULATION FOR CONCEPT VIC
REGENERATIVE LIQUID PROPELLANT GUNS,
I. 30 MM

TERENCE P. COFFEE
GLORIA P. WREN
WALTER F. MORRISON

DTIC
ELECTE
MAR 0 1 1990
S B D

DECEMBER 1989

U.S. ARMY LABORATORY COMMAND

BALLISTIC RESEARCH LABORATORY
ABERDEEN PROVING GROUND, MARYLAND

29 045

DESTRUCTION NOTICE

UNCLASSIFIED

REPORT DOCUMENTATION PAGE		Form Approved OMB No. 0704-0188

1a. REPORT SECURITY CLASSIFICATION UNCLASSIFIED	1b. RESTRICTIVE MARKINGS

2a. SECURITY CLASSIFICATION AUTHORITY	3. DISTRIBUTION/AVAILABILITY OF REPORT
2b. DECLASSIFICATION/DOWNGRADING SCHEDULE	Approved for public release; distribution is unlimited.

4. PERFORMING ORGANIZATION REPORT NUMBER(S) BRL-TR-3072	5. MONITORING ORGANIZATION REPORT NUMBER(S)

6a. NAME OF PERFORMING ORGANIZATION Ballistic Research Laboratory	6b. OFFICE SYMBOL (If applicable) SLCBR-IB-B	7a. NAME OF MONITORING ORGANIZATION

6c. ADDRESS (City, State, and ZIP Code) Aberdeen Proving Ground, MD 21005-5066	7b. ADDRESS (City, State, and ZIP Code)

8a. NAME OF FUNDING/SPONSORING ORGANIZATION Ballistic Research Laboratory	8b. OFFICE SYMBOL (If applicable)	9. PROCUREMENT INSTRUMENT IDENTIFICATION NUMBER

8c. ADDRESS (City, State, and ZIP Code) Aberdeen Proving Ground, MD 21005-5066	10. SOURCE OF FUNDING NUMBERS			
	PROGRAM ELEMENT NO.	PROJECT NO.	TASK NO.	WORK UNIT ACCESSION NO.

11. TITLE (Include Security Classification)

A Comparison Between Experiment and Simulation for Concept VIC Regenerative Liquid Propellant Guns, I. 30 mm

12. PERSONAL AUTHOR(S)
Terence P. Coffee, Gloria P. Wren, Walter F. Morrison

13a. TYPE OF REPORT Technical Report	13b. TIME COVERED FROM _____ TO _____	14. DATE OF REPORT (Year, Month, Day)	15. PAGE COUNT

16. SUPPLEMENTARY NOTATION

17. COSATI CODES			18. SUBJECT TERMS (Continue on reverse if necessary and identify by block number)
FIELD	GROUP	SUB-GROUP	liquid monopropellant, concept VIC
			regenerative gun, lumped parameter model
			liquid propellant guns,

19. ABSTRACT (Continue on reverse if necessary and identify by block number)

Regenerative liquid propellant gun (RLPG) technology is sufficiently mature to allow the testing of the first 155-mm liquid propellant gun. In support of the development of this artillery weapon, test fixtures in 30-mm and 105-mm sizes have been built and fired. This report describes the analysis and modeling of the 30-mm gun fixture. Future reports will concentrate on the 105-mm and 155-mm guns. The Concept VIC gun design is described. The basic assumptions in the numerical lumped parameter model are described. Modifications to the model required by the VIC gun are given. There is a brief discussion of the 30-mm test program. The model is first benchmarked against a series of medium charge firings. These are the best characterized set of experiments, with the best reproducibility. The process of choosing input values for the gun code is discussed in detail. The result is excellent agreement with all of the experimental data. The model is then used to predict the performance of some of the short-charge firings. The muzzle velocities are predicted very accurately. The pressure profiles are not. The reasons for the lack of agreement in the pressure profiles are discussed.

20. DISTRIBUTION/AVAILABILITY OF ABSTRACT ☐ UNCLASSIFIED/UNLIMITED ☒ SAME AS RPT. ☐ DTIC USERS	21. ABSTRACT SECURITY CLASSIFICATION UNCLASSIFIED
22a. NAME OF RESPONSIBLE INDIVIDUAL Terence P. Coffee	22b. TELEPHONE (Include Area Code) (301)-278-6169	22c. OFFICE SYMBOL

DD Form 1473, JUN 86   *Previous editions are obsolete.*   SECURITY CLASSIFICATION OF THIS PAGE

UNCLASSIFIED

INTENTIONALLY LEFT BLANK.

TABLE OF CONTENTS

INTENTIONALLY LEFT BLANK.

LIST OF FIGURES

LIST OF FIGURES (Continued)

LIST OF TABLES

INTENTIONALLY LEFT BLANK.

ACKNOWLEDGMENTS

Intentionally left blank.

1. INTRODUCTION

Regenerative liquid propellant gun (RLPG) technology is sufficiently mature to allow the testing of the first 155 mm liquid propellant gun. In support of the development of this artillery weapon, test fixtures in 30 mm and 105 mm sizes have been built and fired. The data from all three of these fixtures have been extensively analyzed to better understand the RLPG process. This paper reviews the 30 mm data for the Concept VIC configuration, the design chosen for the 155 mm gun, and examines the modeling of that system. Future papers will focus on 105 mm and 155 mm data.

The structure for the modeling effort discussed in this paper is dictated by the proposed transition of the LP program from the Ballistic Research Laboratory (BRL) to the Army Research, Development, and Engineering Center (ARDEC). The transition criteria specify that it should be possible to demonstrate agreement between model and test data for 30 mm, 105 mm, and 155 mm, by matching mean, filtered pressure-time data to within 5 percent in pressure for damper, reservoir, chamber, and bore, and by matching muzzle velocity to within 2 percent.[1] In addition, it was desired to extend the modeling exercise by attempting to predict performance of different charge sizes based on a calibration of model parameters.

This report documents the modeling of the 30 mm Concept VIC data. First, a description of the Concept VIC fixture is given. The gun code utilized has been described in previous publications,[2,3] with modifications pertinent to the Concept VIC design described in detail in this paper. The choice of input parameters is also described, most of which are determined from the physical characteristics of the gun. However, some parameters cannot be determined directly and are chosen based on empirical evidence. A series of shots, referred to as the repeatability series, is used to meet the transition criteria and to calibrate the code. Once the baseline parameters have been chosen, these values are used to predict the performance of different charge sizes. In general, the predictions are reasonable.

2. THE CONCEPT VIC LIQUID PROPELLANT GUN

A diagram of a VIC liquid propellant gun (initial position) is shown in Figure 1. The liquid propellant (LP) in the reservoir is between the control piston and the outer injection piston. A primer is ignited and injects hot gas into the combustion chamber. As the chamber is pressurized, the control piston (or control rod) is pushed to the left, opening an injection vent. The outer piston will follow the control rod, actually injecting the propellant. Figure 2 shows the gun part way through the injection process, and Figure 3 shows the gun at the end of stroke.
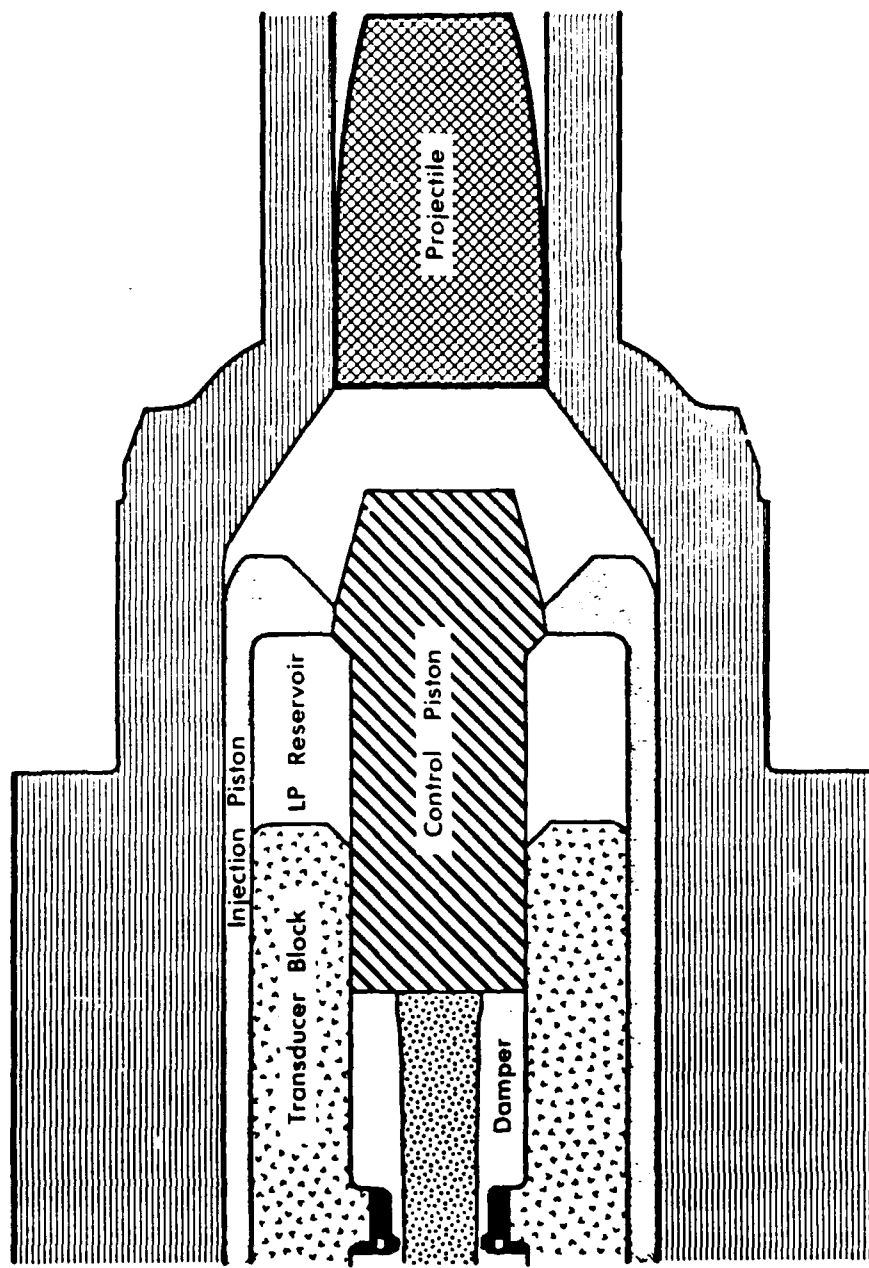
Figure 1. A Concept VIC Regenerative Liquid Propellant Gun, Initial Position.

2
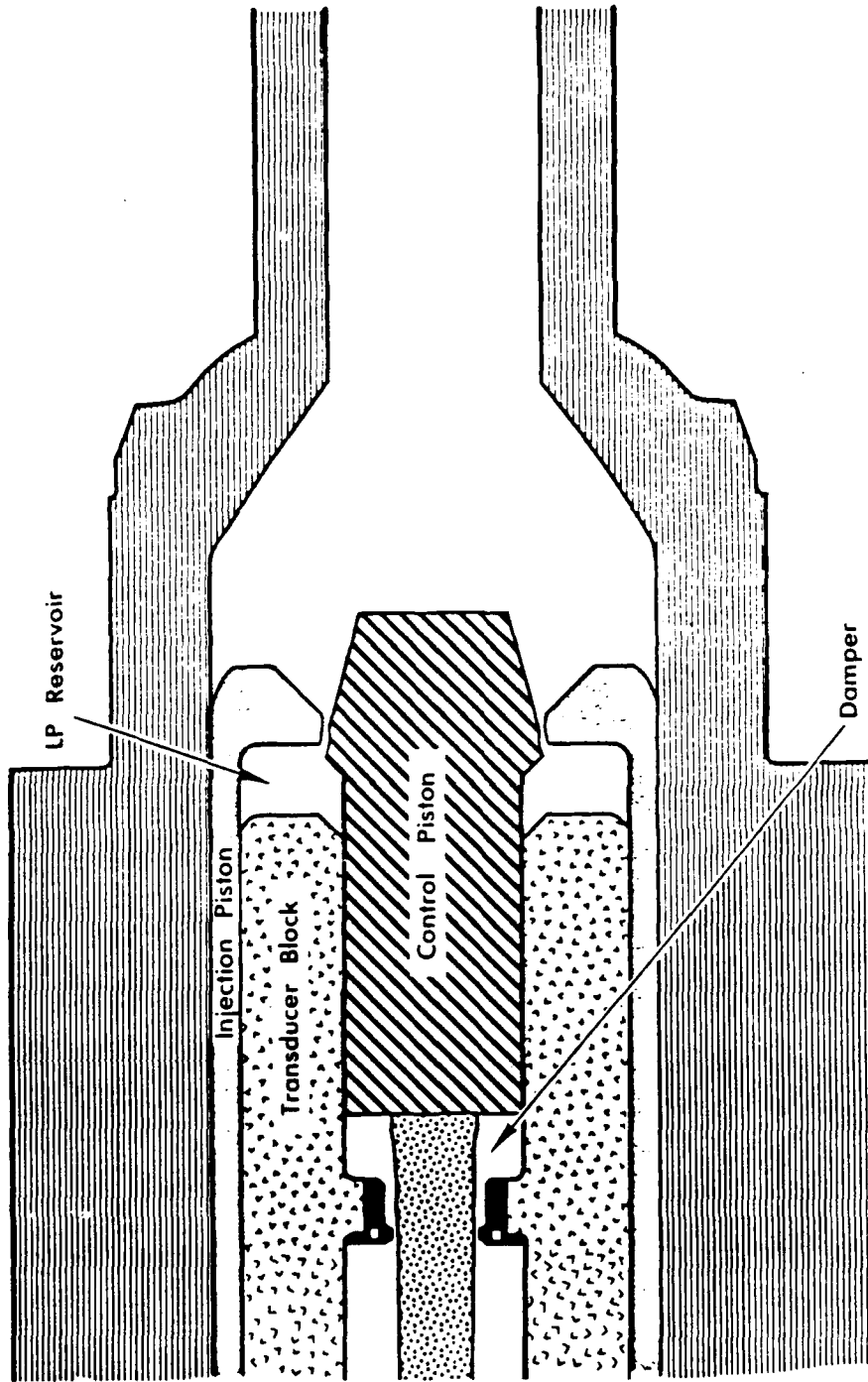
Figure 2. A Concept VIC Regenerative Liquid Propellant Gun, Middle of Stroke.

3
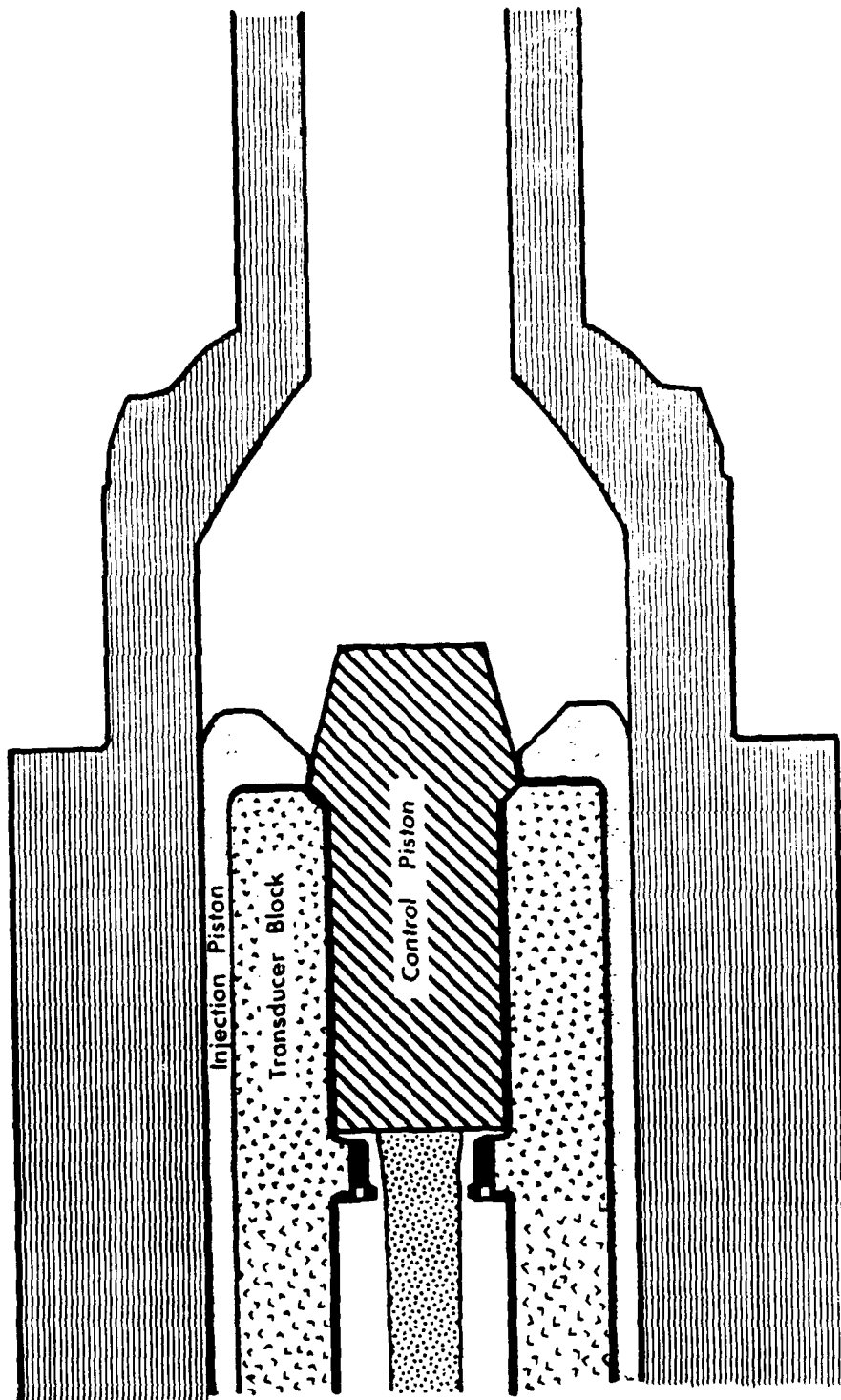
Figure 3. A Concept VIC Regenerative Liquid Propellant Gun, End of Stroke.

Injection Piston

Transducer Block

Control Piston

4

The motion of the control piston depends upon the damper assembly. After the initial seal is broken, the liquid pressure has very little effect on this piston. There is damper fluid initially between the transducer block and the damper rod attached to the back of the control piston. As the control piston moves, damper fluid is forced between the rod and the extension on the transducer block. Two flat areas are machined on the rod to control the vent area. Near the end of stroke, the damper vent area becomes small, restricting the outflow of damper fluid and, thus, acting to decelerate the control rod, bringing it to a gradual halt.

The injection piston will track the control rod in response to the differential pressure in the liquid reservoir and the combustion chamber. As the piston moves close to the control rod, the vent area will decrease, the liquid pressure will increase, and the piston will slow down. As the piston moves further from the rod, the vent area will increase, the liquid pressure will decrease, and the piston will accelerate.

The fixture utilized in the firings discussed in this report was designed, fabricated, and fired under contract by General Electric (GE).

3. BASIC ASSUMPTIONS

The propellant in the liquid reservoir is assumed to be a homogeneous, compressible, isothermal fluid. The mass flux out of the reservoir is computed assuming steady-state Bernoulli flow. Similarly, the liquid in the damper is assumed to be a homogeneous, compressible, isothermal fluid. The flow through the damper orifice is computed also assuming steady-state Bernoulli flow.

The combustion chamber fluid is assumed to be homogeneous and stagnant. As a first approximation, the liquid is assumed to combust instantaneously upon entering the combustion chamber, releasing all its energy. Alternately, the liquid can be assumed to instantaneously form droplets of a given size, which burn depending upon a pressure dependent burning law.

The primer is assumed to be the same material as the propellant. The primer gases are injected at a steady rate over a given time period. Since actual primer gases are injected through a long, narrow tube and show large heat losses, some percentage of the energy of the primer may be assumed to be lost in this injection process.

5

The mass flux into the gun tube is computed assuming steady-state isentropic flow. The gun tube is modeled using a modification of the Lagrange pressure distribution.

4. GOVERNING EQUATIONS

With the above assumptions, the regenerative gun behavior can be modeled by 18 ordinary differential equations (assuming instantaneous burning). These equations are marked using numbers in square brackets at the left ([1] to [18]). The equations are given below for a concept VIC gun. Only those equations that are modified from the previous report are discussed in detail.[3] The equations describe the four lumped parameter regions (liquid reservoir, combustion chamber, gun tube, and damper), the mass flux between the regions, and the motion of the control piston, outer piston, and projectile. For historical reasons, the reservoir is numbered 1, the chamber is numbered 3, and the gun tube is numbered 4. A concept called a reverse annular gun has an additional region, the intermediate chamber, numbered 2. The damper region is numbered 5. If droplet formation and combustion are assumed, the equations become considerably more complicated.

4.1 Liquid Reservoir and Outer Piston. The equation governing the volume of the liquid reservoir is fairly complicated for the concept VIC configuration. The boundary between the liquid reservoir and the combustion chamber is the point on the outer piston (also called the injection piston) where the outer piston and the inner piston (also called the control rod) initially meet. This will normally be the minimum area of the orifice. The differences in the location, s_{mv}, and speed, v_{mv}, of the two pistons are considered. Let

$$s_{mv} = s_{pt} - s_{rd} \tag{1}$$

and

$$v_{mv} = v_{pt} - v_{rd}, \tag{2}$$

where s_{pt} is the outer piston travel, v_{pt} is the outer piston velocity, s_{rd} is the control rod travel, and v_{rd} is the control rod velocity. The rod radii are read in as a table. At any given time step, the relative piston travel is between two input distances, x_{i-1} and x_i, i.e., the position of the point of minimum radius on the injection piston in the coordinate system affixed to the control rod is between x_{i-1} and x_i (see Figure 2). The radius of the central bolt, r, at this point is found by linear interpolation

$$r = r_{i-1} + \frac{(s_{mv} - x_{i-1})}{(x_i - x_{i-1})} (r_i - r_{i-1}). \tag{3}$$

The vent area is then given by

$$A_v = A_h - \pi r^2 , \qquad (4)$$

where A_h is the constant area of the opening formed by the outer piston.

The volume of the liquid reservoir can now be discussed. As the outer piston moves, the rate of change of the volume inside this piston is given by $-v_{ps} A_1$, where A_1 is the total area inside the piston. That is, A_1 is the area from the center line to the inside of the injection piston, including the area of the control piston (see Figure 1). This must be corrected by the change in the volume of the control rod in the reservoir. As the control rod withdraws into the transducer block, the rate of change of the volume is given by $v_{rd} A_e$, where A_e is the cross-sectional area of the control rod at the transducer block end of the liquid reservoir. The control rod may also be moving into or out of the reservoir at the combustion chamber end, due to the motion of the control rod relative to the outer piston. The volume change here depends on the derivative of the radius of the rod under the vent

$$\frac{dr}{dt} = v_{mv} \frac{(r_i - r_{i-1})}{(x_i - x_{i-1})} . \qquad (5)$$

After some algebra utilizing the volume of the frustum of a cone, the rate of change of the volume due to the relative motion of the pistons is

$$V_{mv} = \frac{\pi}{3} [v_{mv} (r^2 + r\, r_{i-1} + r_{i-1}^2) + (s_{mv} - x_{i-1})(2r + r_{i-1}) \frac{dr}{dt}] . \qquad (6)$$

The equation for the rate of change of the volume of the liquid reservoir is then

[1]
$$\frac{dV_1}{dt} = -v_{ps} A_1 + v_{rd} A_e + V_{mv} . \qquad (7)$$

The rate of change of the volume depends on the velocity of the injection piston, the velocity of the control rod, and the relative velocity of the pistons.

7

Equations [2] and [3] for the acceleration and travel of the outer piston are unchanged from the previous report.[3] The acceleration of the piston equals the force on the piston divided by the mass of the piston. That is,

$$[2] \qquad \frac{dv_{ps}}{dt} = \frac{g_o}{M_{ps}} [p_3 (A_3 - A_h - A_g) - (p_1 + p_{ps}) (A_1 - A_h)] , \qquad (8)$$

where A_3 is the area of the combustion side of the piston, A_g is the area of the grease dyke, p_1 is the pressure in the liquid chamber, p_3 is the pressure in the combustion chamber, and M_{ps} is the mass of the piston. The grease dyke is the volume between the injection piston and the chamber wall. Measurements indicate that the grease trapped in this volume has a pressure very near to the combustion chamber pressure. So rather than including in the code a model of the grease dyke, it is assumed to be at the pressure p_3. The quantity $g_o = 10^7$ g/s-cm-MPa is a conversion constant to put the acceleration in the desired units of cm²/s. The quantity p_{ps} is an empirical correction to simulate the effects of frictional resistance. The equation governing the piston travel is

$$[3] \qquad \frac{ds_{ps}}{dt} = v_{ps} . \qquad (9)$$

The equations for the liquid density and pressure in the reservoir are likewise unchanged. From conservations of mass,

$$[4] \qquad \frac{d\rho_1}{dt} = - \frac{\rho_1}{V_1} \frac{dV_1}{dt} - \frac{m_{13}}{V_1} , \qquad (10)$$

where ρ_1 is the density of the liquid and m_{13} is the mass flow rate out of the reservoir. The energy equation can be written as

$$[5] \qquad \frac{dp_1}{dt} = \frac{c_1^2}{g_o} \frac{d\rho_1}{dt} , \qquad (11)$$

where c_1 is the speed of sound in the liquid.

The mass flow out of the reservoir is assumed to be steady-state Bernoulli flow

$$m_{13} = C_D A_v \sqrt{2g_o \rho_1 (p_1 - p_3)} . \qquad (12)$$

8

The discharge coefficient C_D is an empirical correction to the equations to take into account frictional losses.

4.2 **Combustion Chamber.** By analogy with equation [1], the rate of change of volume of the combustion chamber is given by

[6]
$$\frac{dV_3}{dt} = v_{ps} A_3 - V_{mv} ,$$
(13)

where V_3 is the volume of the combustion chamber, and A_3 is the area of the combustion side of the piston (including the central hole). The equations for the density [7] and pressure [8] are unchanged. From conservation of mass,

[7]
$$\frac{d\rho_3}{dt} = -\frac{\rho_3}{V_3} \frac{dV_3}{dt} + \frac{m_{13} - m_{34}}{V_3} + \frac{m_{p3}}{V_3} ,$$
(14)

where ρ_3 is the density of the gas in the combustion chamber, and m_{34} is the mass flux into the gun tube; m_{p3} is the rate at which primer gas is injected into the chamber. The energy equation is

[8]
$$\frac{dp_3}{dt} = \frac{c_3^2}{g_o} \frac{d\rho_3}{dt} + \frac{m_{13} (h_{L1} - h_{G3}) (\gamma - 1)}{V_3 - b M_3}$$
$$+ \frac{m_{p3} (e_1 - h_{G3}) (\gamma - 1)}{V_3 - b M_3} ,$$
(15)

where c_3 is the speed of sound in the chamber, h_{L1} is the enthalpy of the liquid, h_{G3} is the enthalpy of the combustion chamber gas, and e_1 is the internal energy of the primer (assumed the same as the liquid propellant). The internal energy, e_1, in this equation may be reduced to simulate heat loss in the primer injection process.

4.3 **Gun Tube and Projectile.** The tube region is unaffected by the changes in the model. The volume has the standard equation

[9]
$$\frac{dV_4}{dt} = v_{pj} A_4 ,$$
(16)

where v_{pj} is the velocity of the projectile, and A_4 is the area of the gun tube. The pressure, p_R, at the base of the projectile is obtained from a modification of the Lagrange pressure gradient. The acceleration equation for the projectile is

[10]
$$\frac{dv_{pj}}{dt} = (p_R - p_{pj}) \, A_4 \, g_o \, / \, M_{pj} \, . \tag{17}$$

As with the piston, the pressure p_{pj} is only a resistive pressure. The projectile travel s_{pj} is given by

[11]
$$\frac{ds_{pj}}{dt} = v_{pj} \, . \tag{18}$$

The last two differential equations are exactly analogous to the combustion chamber equations. That is,

[12]
$$\frac{d\rho_4}{dt} = - \frac{\rho_4}{V_4} \, \frac{dV_4}{dt} + \frac{m_{34}}{V_4} \, , \tag{19}$$

where ρ_4 is the space mean average density of the gas in region 4, and

[13]
$$\frac{dp_4}{dt} = \frac{c_4^{\,2}}{g_o} \, \frac{d\rho_4}{dt} + \frac{m_{34} \, (h_{G3} - h_{G4}) \, (\gamma - 1)}{V_4 - b \, M_4}$$
$$- \frac{Q_w \, (\gamma - 1)}{(1 - b\rho_4)} \, . \tag{20}$$

Q_w represents the heat loss to the gun tube walls. The mass flow into the gun tube is derived assuming isentropic expansion of the gas into the gun tube throat. The throat conditions are denoted by the subscript t. The resulting equation is

$$v_t = \sqrt{2g_o \, \{b(p_3 - p_t) + c_p T_t \, [(p_3 \, / \, p_t \,)^{(\gamma-1)/\gamma} - 1]\}} \, , \tag{21}$$

where v_t is the gas velocity at the gun tube throat, b is the covolume of the gas, and γ is the ratio of specific heats. The actual mass flow rate into the tube is

$$m_{34} = C_D{}' \, A_4 \, \rho_t \, v_t \, . \tag{22}$$

The discharge coefficient $C_D{}'$ is as before an empirical correction for loss terms. This is usually set to one.

4.4 Damper and Control Rod. The damper vent area is read in as a table of area versus control rod travel. The vent area, A_{v5}, at any given time is found by interpolation. Let A_{r5} be the area of the control rod (damper end). Let A_{h5} be the area of the hole in the block assembly. Then the liquid area at the vent exit is

$$A_{x5} = A_{r5} - A_{h5} + A_{v5} \ . \tag{23}$$

This is the area that the damper pressure will act upon.

Let A_{mx} be the maximum cross-sectional area of the control rod, which corresponds to the position of maximum radius of the control rod. Before the pistons start to move, the acceleration on the rod is given by

[14]
$$\frac{dv_{rd}}{dt} = \frac{g_o}{M_{rd}} \ [p_3 \ A_h - p_1 \ (A_{mx} - A_e) - p_5 \ A_{x5}] \ , \tag{24}$$

where M_{rd} is the mass of the control rod, and p_5 is the pressure in the damper. After the rods separate, the liquid pressure will act on the bolt up to the vent opening. By assumption, the transition from liquid to chamber pressure is a discontinuity at the vent. Then

[14]
$$\frac{dv_{rd}}{dt} = \frac{g_o}{M_{rd}} \ [p_3 \ A_{rv} + p_1 \ (A_e - A_{rv}) - p_5 \ A_{x5}] \ , \tag{25}$$

where A_{rv} is the area of the control rod at the vent. In present designs, A_e is only slightly larger than A_{rv}, so the liquid pressure has very little effect on the motion of the control rod. The equation for the control rod travel is

[15]
$$\frac{ds_{rd}}{dt} = v_{rd} \ . \tag{26}$$

The rate of change of the volume can be represented by

[16]
$$\frac{dV_5}{dt} = - v_{rd} \ A_{x5} \ . \tag{27}$$

The above equation simply represents the liquid area at the vent end of the damper multiplied by the control rod velocity.

11

By analogy to the liquid reservoir equations, the density equation is

[17]
$$\frac{d\rho_5}{dt} = - \frac{\rho_5}{V_5} \frac{dV_5}{dt} - \frac{m_5}{V_5} ,$$
(28)

where ρ_5 is the density of the damper fluid, and m_5 is the mass flux out of the damper (computed assuming steady-state Bernoulli flow). The pressure equation is

[18]
$$\frac{dp_5}{dt} = \frac{c_s^2}{g_o} \frac{d\rho_5}{dt} ,$$
(29)

where c_5 is the speed of sound in the liquid.

5. CODE MODIFICATIONS

A number of changes were made to the gun code to handle the Concept VIC guns. The new subroutines added are described below, as are the major changes in the old subroutines. The appropriate set of options is chosen by the user. The code then calls a subroutine of the same name to implement the choice.

5.1 VENT4. This option is for a VIC type outer piston and control rod injector. A table of control rod radius versus relative piston travel is read in. The area of the hole in the outer piston and the grease dyke is read in. The weight of the control rod is input.

The subroutine, VENT4, then computes at each time step the vent area, the time rate of change of the reservoir and chamber volumes, and the acceleration of the outer piston and the control rod. A damper option must also be chosen to obtain the parameters for the forces on the damper side of the control rod.

5.2 BUFF2. This option was originally designed for a Concept VIA gun in which only the outer piston moved, and the damper (or buffer) slowed the piston at the end of stroke. The option was generalized to include the VIC gun in which the damper pressure acts on the inner piston during the entire injection cycle. The damping fluid is usually water or Brayco 783.

The area of the control rod (damper side) and the area of the opening formed by the bushing on the transducer block are read in. If the constant hole area is greater than zero, a VIC fixture is

12

assumed. A discharge coefficient, which is assumed to be constant throughout the firing cycle, is input. The initial volume and pressure of the damper, as well as the pressure of the region that the damper will be injecting into, are input. For the VIC gun, these two pressures are the same. The density at atmospheric pressure, the bulk modulus, and the pressure derivative of the bulk modulus are given. Since there have been concerns about ullage in the damper, it is possible to specify that some part of the initial volume is gas. Finally, the vent area as a function of control rod travel is specified.

At any given time step, the subroutine computes the vent area, the liquid area at the vent, and the sound speed. The actual time derivatives for the damper volume, density, and pressure are in the routines FDROP1 (instantaneous burning) or FDROP2 (droplet burning).

In this fixture, there is a small hole drilled in the damper to help relieve initial ullage. The area of this hole is also read in and added to the annular vent area around the bolt when the mass flux out of the damper is computed.

5.3 BUFF3. There is an option to use experimental values for the damper pressure rather than to compute the pressure. This is similar to the option CHAM2 for chamber pressure. The purpose is to use the experimental values for boundary conditions and determine if the piston motion submodel then will agree with the experiment.

5.4 BUFF4. The time derivative of the damper pressure, rather than the pressure itself, is read in. The time derivative is found numerically. These values then override the time derivatives computed by the above set of equations. This is more stable than the BUFF3 option and usually runs faster, although the results are the same.

5.5 CHAM3. The CHAM2 option used the experimental chamber pressure as a boundary condition. This new option reads in the time derivative profile of the experimental chamber pressure instead. As in the damper options, this leads to a decrease in the run time for the code.

5.6 PRIM3. This option has been modified to include a heat loss fraction. Since the primer gas is normally injected through a long, narrow tube, heat loss can be substantial. Previously, this was taken into account simply by using less primer. Instead, the chemical energy of the primer is now multiplied by a heat loss fraction. This allows the proper mass to be injected while still adjusting the pressure caused by the primer.

5.7 <u>DROP4</u>. The droplet size previously was allowed to vary with the piston travel (DROP3). But for the VIC gun, injection is more complicated and depends on the motion of both pistons. Instead, the droplet size can be read in as a function of maximum chamber pressure. After the chamber pressure reaches its maximum and starts to decrease, the droplet diameter will remain at its last size.

6. 30 MM CONCEPT VIC DATA

The 30 mm Concept VIC RLPG was tested using LGP1846 to evaluate the concept's performance using different charge lengths and initial chamber volumes in preparation for implementing the concept in a 155 mm RLPG.[4] Three different configurations were tested: (1) 94 cc liquid propellant charge and 280 cc initial combustion chamber volume; (2) 94 cc liquid propellant charge and 747 cc initial combustion chamber volume; and (3) 230 cc liquid propellant charge and 500 cc initial combustion chamber volume. Projectile weights ranged from 679 g to 682 g. The igniter used was IMR 4350 solid propellant and an M52 primer cap. A brief summary of the main test series is given in Table 1. Only the cases in which the same configuration was fired successfully in a series of shots are given. The average muzzle velocity for the series is given, along with the standard deviation (S.D.) in muzzle velocity. The last test series (tests 39, 42-49, and 51) is referred to as the repeatability series.

TABLE 1. 30 mm Concept VIC Test Results.

Test	Liquid volume, cc	Chamber volume, cc	Velocity, m/s	S.D., %
12-17	94	280	622.0	0.72
18-23	94	747	546.5	1.17
28-29, 31-38	230	500	773.0	0.50
39, 42-49, 51	230	500	776.0	0.39

Care was taken in the repeatability series to isolate the variations in gun performance from the variations in propellant lots and projectile weights. The propellant used throughout the series was taken from the same lot, and the projectiles, except for the last test, weighed within 0.16 g of each other. No hardware changes were made that would alter the ballistic performance of the gun. The results indicate excellent repeatability in muzzle velocity.

In general, GE concluded that the Concept VIC, 30 mm RLPG demonstrated excellent performance, and the VIC concept has the potential for providing excellent performance in the 155 mm RLPG. The hardware was in good condition at the completion of the tests. The same outer and inner pistons were used in all of the tests performed.

7. GE 30 MM GUN FIXTURE - BASELINE

The best characterized 30 mm Concept VIC experiments are the medium charge repeatability tests (shots 39-51). The mean muzzle velocity for this series of tests is 776 m/s with a standard deviation of 0.39 percent. Although the muzzle velocity repeatability is good, the pressure measurements show inaccuracies. The chamber pressure for two shots at two gauge locations is shown in Figure 4. The gauge locations are in the same plane near the front of the combustion chamber, and the pressures should be nearly the same, particularly since the muzzle velocity for the two shots is almost identical. Figure 5 shows a similar picture for the liquid pressure for the same two shots from gauges in the same plane. It appears that there are calibration problems with the gauges, and the actual maximum pressures are not known.

Figure 6 compares the damper pressures for the two shots. There is only one gauge in the damper area, and the agreement is better than for the liquid and chamber pressures. Figure 7 shows the travel for the control rod and the outer piston, and the agreement here is good. Moreover, the piston travel is measured directly with an optron, and the measured end of stroke agrees very well with the actual stroke of the hardware.

For this particular shot, the radar signal was digitized at a rate twice as fast as the other data. The data window received at BRL did not show the radar trace for the entire firing cycle, and only the first part of the projectile travel could be derived (see below). However, other complete radar traces have shown radar dropout at several points through the cycle. Normally, only the beginning of the projectile travel can be recovered, so the partial loss of data is not considered important.

Most of the parameters for the gun code are based on physical measurements of the gun fixture or known propellant or damper fluid properties (Appendix A). However, some of the parameters cannot be predicted, and the values must be selected based on the experimental data. One parameter that has been studied in the past is the discharge coefficient for the flow out of the liquid reservoir. This can be derived from the experimental chamber and liquid pressures and the experimental piston travels using an inverse code.[5,6] The higher of the pressure profiles for each round shown in Figure 4 was used to determine the discharge coefficient (see below). When the
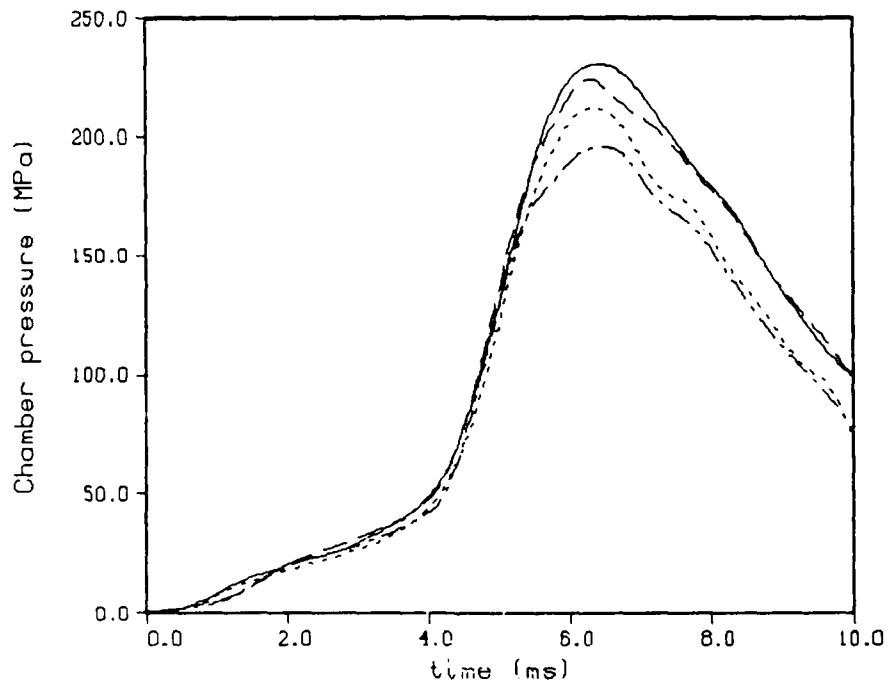
Figure 4. Experimental Chamber Pressure. Round 51 - Gauge F30 (line) and Gauge F120 dot). Round 48 - Gauge F30 (dash) and Gauge F120 (dot-dash).

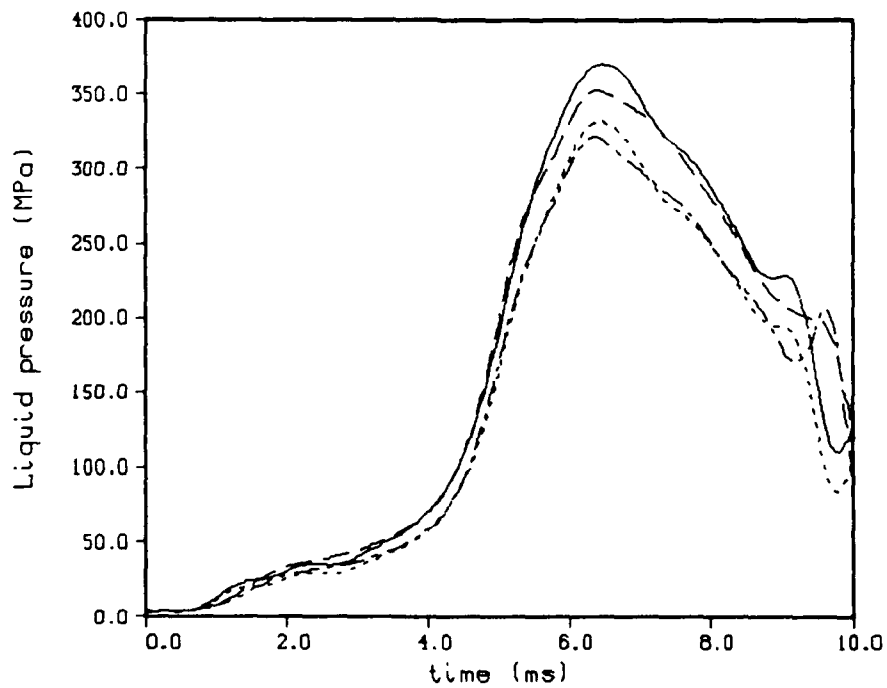

Figure 5. Experimental Liquid Pressure. Round 51 - Gauge LP210 (line) and Gauge LP90 (dot). Round 48 - Gauge LP210 (dash) and Gauge LP90 (dot-dash).
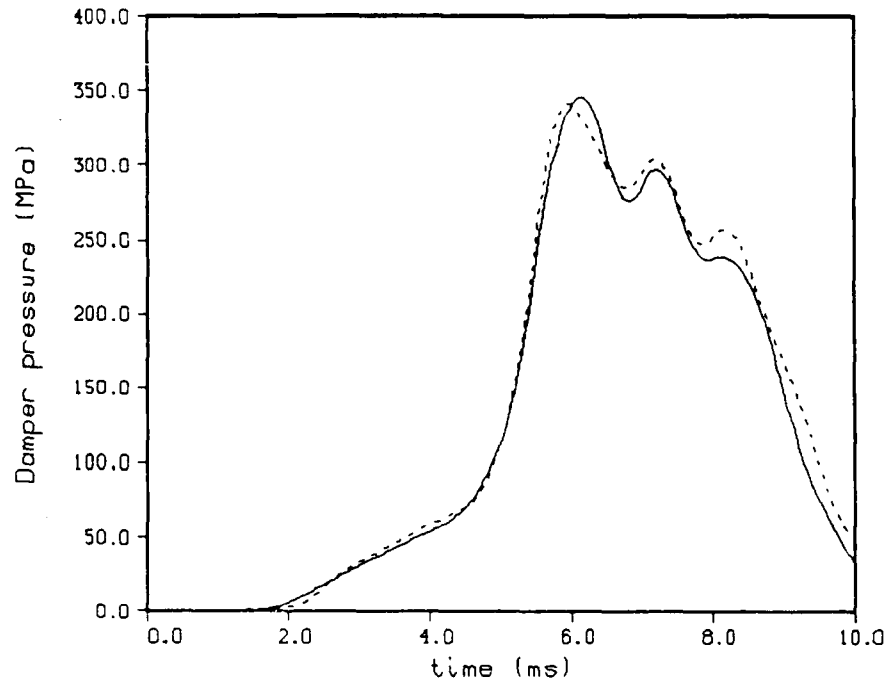
16

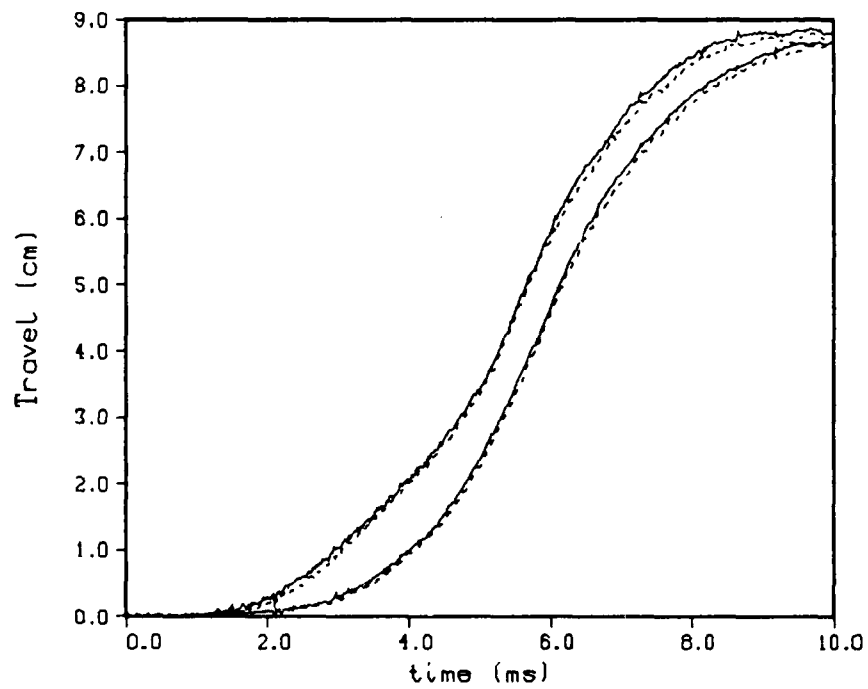Figure 6. Experimental Damper Pressure. Round 51 (line); Round 48 (dot).

Figure 7. Experimental Piston Travels. Round 51 (line); Round 48 (dot).

17

vent area changes rapidly, as is the case here, it is clearer to represent the results in terms of effective area (discharge coefficient times vent area).[7] Figure 8 shows the results for shots 51 and 48.

The solid line represents the physical vent area. The area of the control rod under the outer piston opening can be calculated, knowing the difference in the piston travels. This profile is very noisy near time zero. The outer piston originally rests on a slanted section of the control rod extending about 0.05 cm past the initial piston position. Small errors in either piston travel will then generate a noticeable vent area before the pistons have actually moved. Once piston motion really begins, the outer piston rapidly moves over a flat section on the control rod that is 0.25 cm long. After this section, the outer piston is over another slanted section until the end of stroke. The noise in the piston travels is amplified in the physical area profile.

The effective area actually becomes larger than the physical area just after 4.0 ms. This is possible for unsteady flow. If the outer piston is decelerating, the flow may be above the steady-state value due to inertia. However, at this point, the piston is still accelerating. The phenomena must then be related to some error in the experimental data. At this point there is a reduction in the physical area which has no obvious explanation. This could be due to a small error in either piston travel. The area change between the first area peak (1.63 cm^2) and the subsequent minimum (1.51 cm^2) is caused by a change in piston separation of only 0.066 cm. The other possibility is an error in the pressure measurements. A pressure difference of another 10 MPa between the liquid reservoir and the combustion chamber would reduce the discharge coefficient to one. The experimental pressure curves do have large uncertainties. However, this additional pressure difference would lead to a pressure ratio well above the hydraulic difference, which seems less likely than the occurrence of very small errors in the piston travels. Due to the experimental uncertainties, the results must be seen as more qualitative than quantitative.

The effective area is very close to the actual area throughout the firing cycle, indicating that the flow losses are small. A value of 0.95 is chosen as the discharge coefficient. One-dimensional modeling indicates that this is a good approximation.[8]

A similar analysis can be conducted for the damper flow (Figure 9). After some initial noise, the effective area is well below the actual area, indicating major flow losses. This is reasonable, since the flow is past a sharp corner. Moreover, part of the flow is through a circular hole in the damper region. This has been drilled to reduce initial gas contamination in the damper. A small circular hole is expected to have a small discharge coefficient. This will be a minor effect until
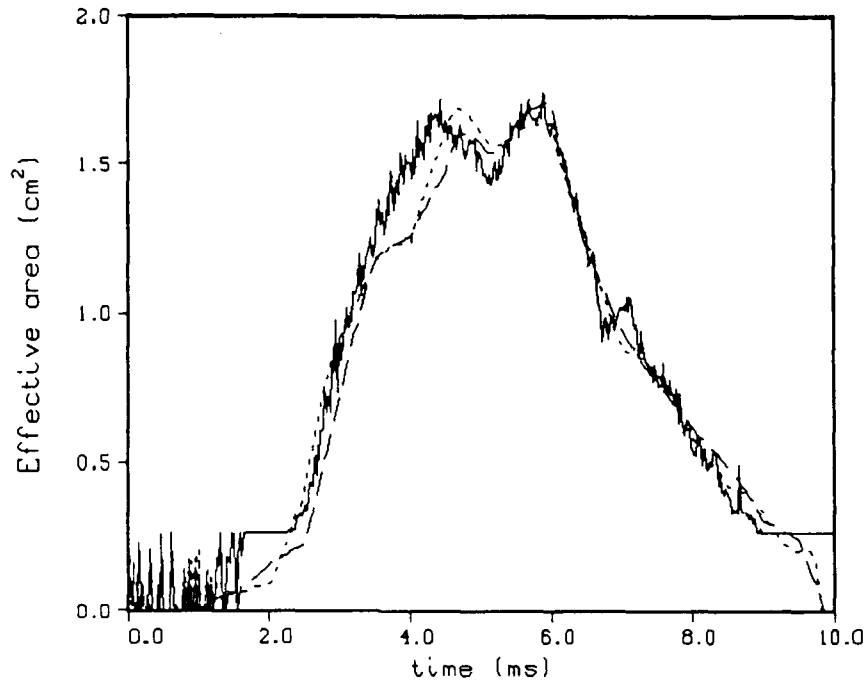
Figure 8. Results From Inverse Code - Reservoir. Injection Area (line). Effective Area - Round 51 (dot) and Round 48 (dash). Based on the Gauges F30 and LP210.
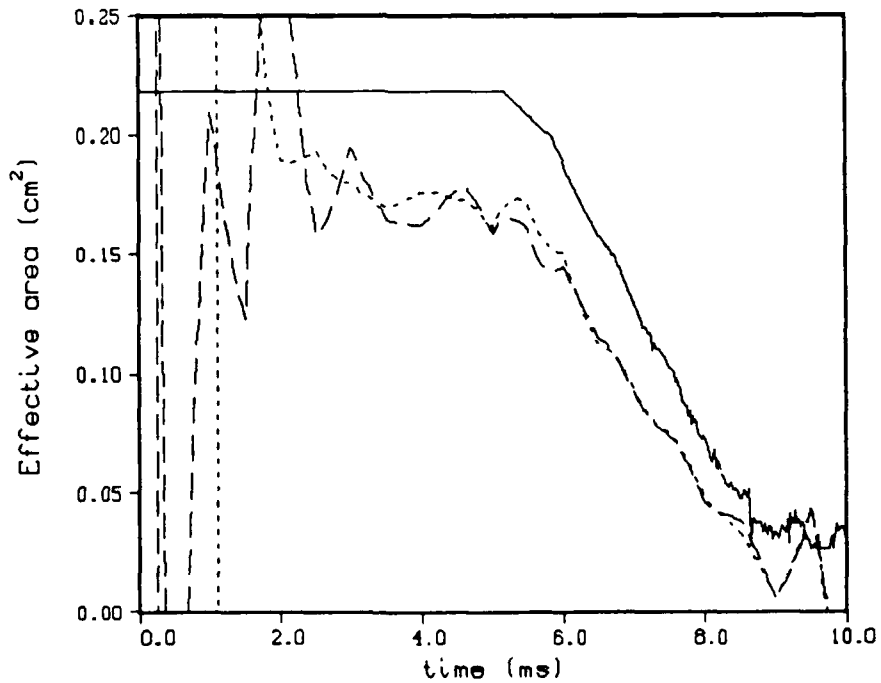

Figure 9. Results From Inverse Code - Damper. Injection Area (line). Effective Area - Round 51 (dot) and Round 48 (dash). Based on the Gauges F30 and LP210.

near the end of the firing cycle, when the hole area is about one-fifth the size of the annular vent around the bolt. The discharge coefficient itself shows a general trend toward smaller values near the end of the firing cycle. It is preferable to use a constant value for the discharge coefficient rather than a profile that changes with time. Therefore, initially an attempt was made to use a constant discharge coefficient. Values between 0.6 and 0.8 seem reasonable.

The ability to use the experimental chamber pressure as a boundary condition was found to be a useful option in the gun code. This allows a check on the piston motion and injection process without having to consider the combustion process. For similar reasons, options were added to read in the experimental damper pressure as a boundary condition (see BUFF3 and BUFF4 options, above).

The code was run using experimental values for both the chamber pressure and the damper pressure. However, the resulting piston travels did not match the experimental travels. The pistons moved much faster in the model run. The problem appears to be that the chamber and damper pressures are closely linked. As the chamber pressure rises, it accelerates the control rod, which raises the damper pressure. This slows down the rod. But when experimental values were used for both pressures, this feedback was lost. Since the pressures are not totally accurate, this was enough to distort the piston travels. Instead, the code was run using only the experimental chamber pressure F30. The damper pressure was predicted by the code. Three different choices for the discharge coefficient out of the damper were made (Figures 10 and 11).

The early damper pressure predicted by the model is different than that in the experimental profile. Moreover, it is almost independent of the choice of discharge coefficient. As the discharge coefficient out of the damper is raised, the control rod moves more rapidly, and keeps the damper pressure up. A discharge coefficient of 0.7 gives a control rod travel that matches the experimental inner piston travel almost exactly. Since only the control rod motion effects the performance of the gun, this agreement is considered satisfactory.

The code was also run using the lower experimental pressure F120 as a boundary condition (Figures 12 and 13). In this case, the model reproduces the early damper pressure more accurately.

Nevertheless, the disagreement in the damper pressures is disturbing. However, since a relatively small change in the chamber pressure leads to a large change in the damper pressure, and since the chamber pressure is not known accurately, this really cannot be examined further. The present, steady-state, Bernoulli flow model with a discharge coefficient of 0.7 is considered an adequate representation.
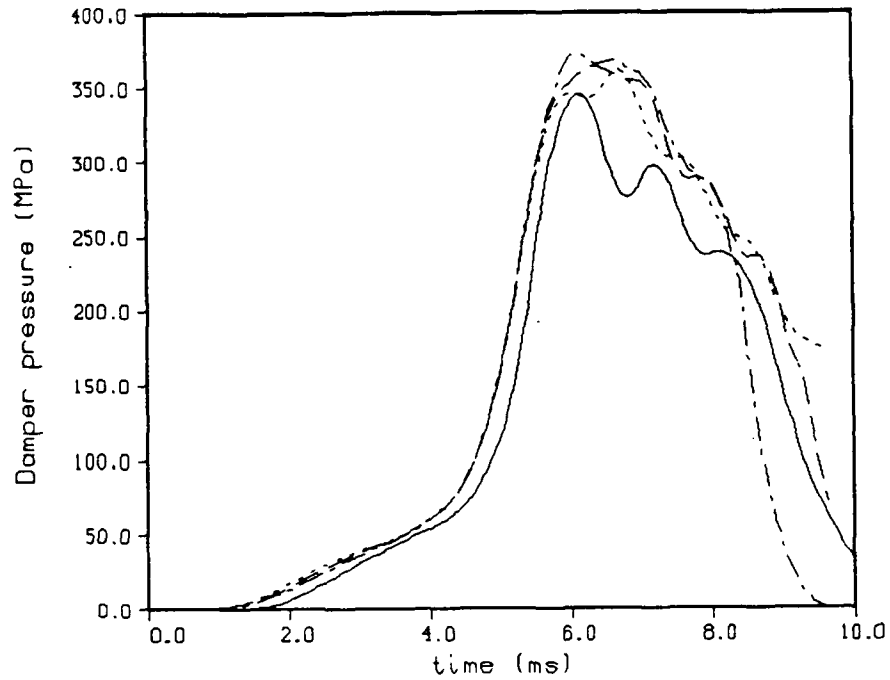
Figure 10. Damper Pressure - Round 51 (line).   Model With Chamber Pressure F30.
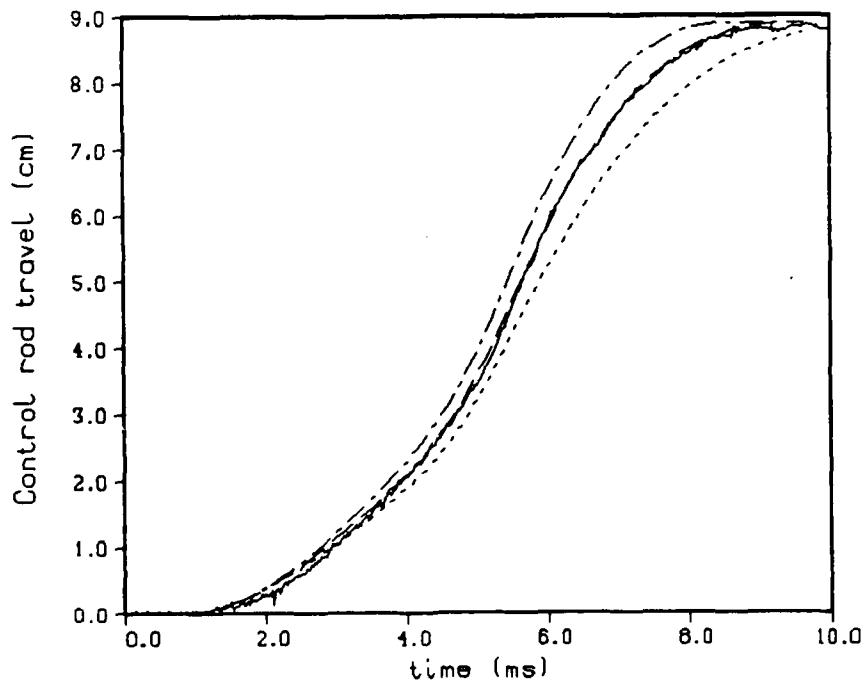$CD_5 = 0.60$ (dot). $CD_5 = 0.70$ (dash). $CD_5 = 0.80$ (dot-dash).

Figure 11. Control Rod Travel - Round 51 (line).   Model With Chamber Pressure F30.
$CD_5 = 0.60$ (dot). $CD_5 = 0.70$ (dash). $CD_5 = 0.80$ (dot-dash).
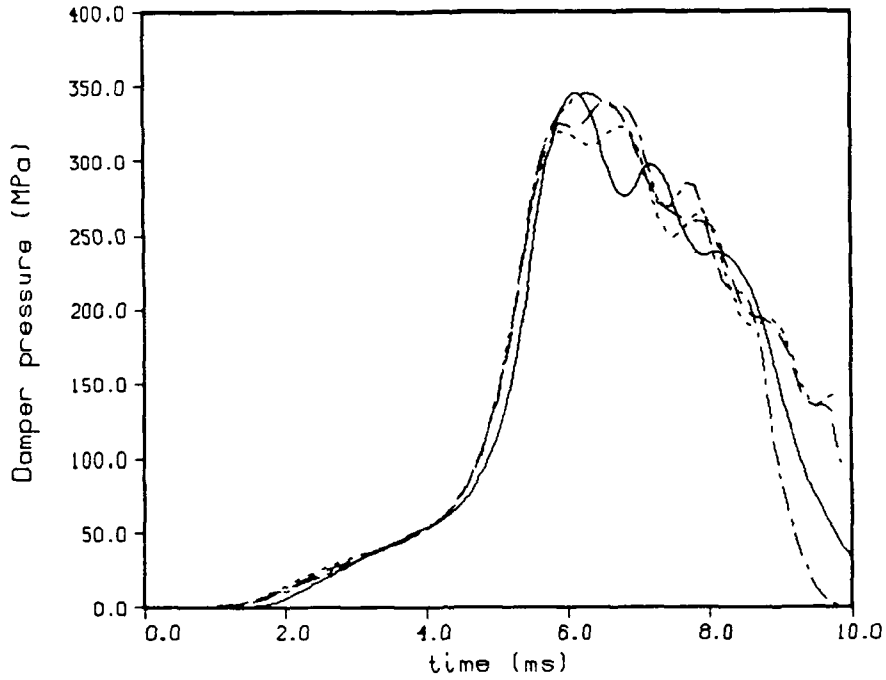
21

Figure 12. Damper Pressure - Round 51 (line). Model With Chamber Pressure F120.
$CD_5 = 0.60$ (dot). $CD_5 = 0.70$ (dash). $CD_5 = 0.80$ (dot-dash).
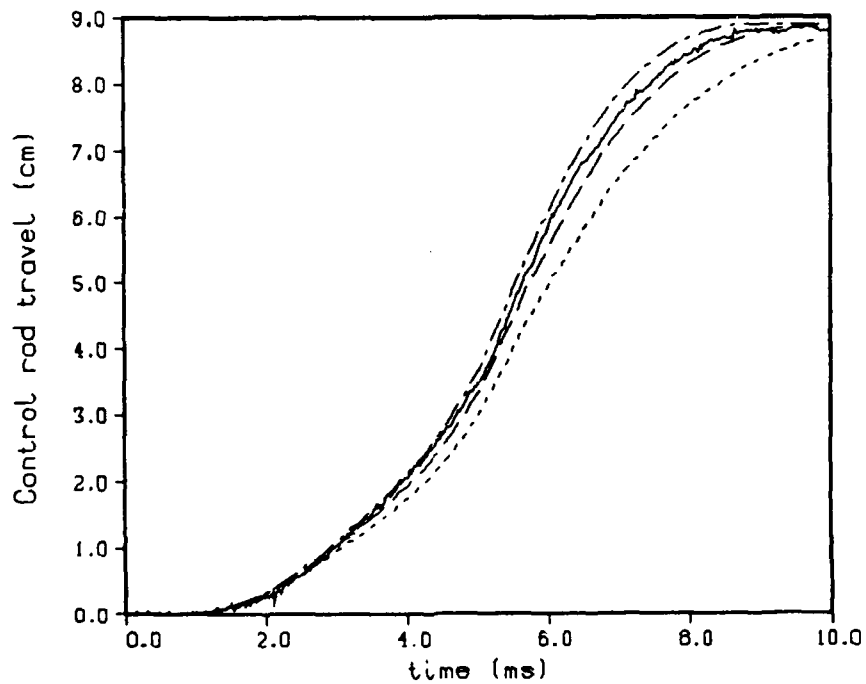

Figure 13. Control Rod Travel - Round 51 (line). Model With Chamber Pressure F120.
$CD_5 = 0.60$ (dot). $CD_5 = 0.70$ (dash). $CD_5 = 0.80$ (dot-dash).

22

The shot start pressure is another important parameter. In the model, the resistance pressure equals the shot start pressure for a distance of one-and-a-half times the length of the engraving band.[9] At this point, the resistance pressure drops off rapidly to a much lower value due to friction. A first estimate of the frictional resistance pressure is 1 percent of the maximum chamber pressure.[9] A value of 2.5 MPa is used in the model.

GE estimates the shot start pressure by looking at the point where the radar trace first shows movement. It estimates a value of 24 MPa for round 51. However, the early projectile motion does not show up well on the radar, and this number is uncertain. Instead, the code is run using the experimental chamber pressure as a boundary condition. The shot start pressure is adjusted until the model matches the early projectile travel.

If the higher pressure F30 is used as a boundary condition, a shot start of 30 MPa represents the early projectile travel almost exactly. The code now predicts a muzzle velocity of 793 ms. This is only slightly higher than the experimental value of 776 ms. If the lower gauge pressure (F120) is used instead, the shot start pressure becomes 24 MPa. This is apparently the profile that GE used in determining the shot start pressure. The muzzle velocity becomes 741 ms. For this reason, the higher pressure is considered to be more accurate.

To remove the reliance on the experimental pressure, the primer model must be set. The experimental primer was adjusted so that the primer provided a chamber pressure rise of about 7 MPa/ms for about 3 ms during water shots. Therefore, the primer was assumed to be injected over a period of 3 ms. The default value of 50 percent heat loss was used. This gives approximately the correct chamber pressure in the absence of liquid propellant combustion in the model.

The remaining element is the combustion chamber model. The simplest approximation is to assume that the liquid combusts instantaneously as it enters the chamber. Results for this model are shown in Figures 14 and 15. A shot start pressure of 30 MPa was used. The pressure rises early, causing the pistons to move too rapidly. In earlier studies,[3] the instantaneous burning option led to pressures higher than the experimental values. Here, the maximum pressure is substantially lower. This indicates that accumulation is important. During the ignition delay, unburnt liquid will accumulate in the chamber. When the injected propellant ignites, it burns off rapidly, leading to a maximum chamber pressure that is higher than predicted using the instantaneous burning option. The predicted muzzle velocity assuming instantaneous combustion is 767 m/s. If the alternate shot start pressure of 24 MPa is used instead, the calculated muzzle velocity is 759 m/s.
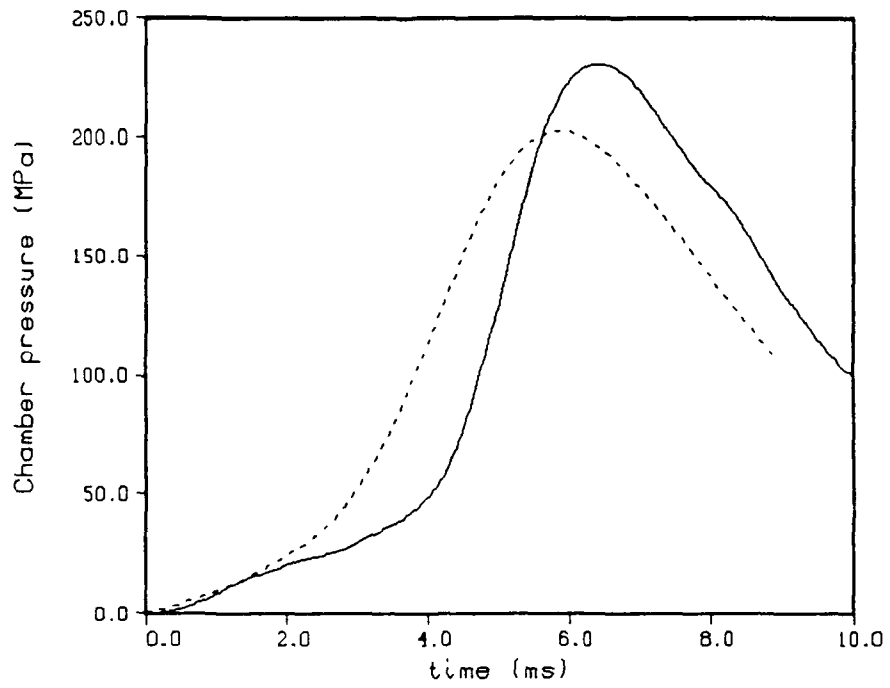
23

Figure 14. Chamber Pressure - Round 51 - Gauge F30 (line). Model With Instantaneous Burning (dot).
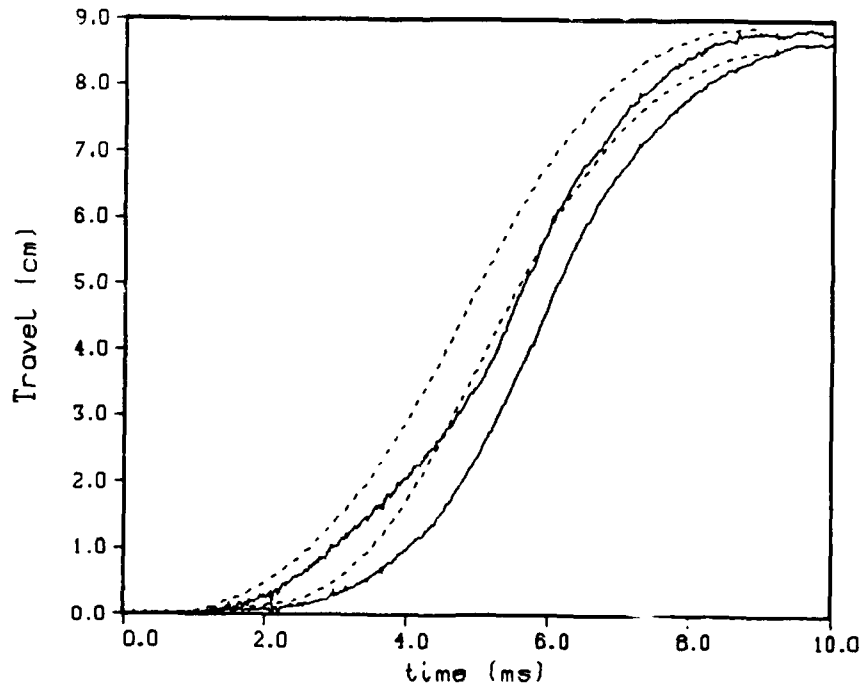

Figure 15. Piston Travels - Round 51 (line). Model With Instantaneous Burning (dot).

24

These results imply the need for a finite rate combustion model. It is assumed that, as the propellant jet enters the combustion chamber, it breaks up into droplets. The number and size of the droplets define a surface area for propellant combustion, and all droplets burn according to a pressure dependent, linear surface regression law that is derived from experimental strand burner data.[10,11] For simplicity, it is assumed that the droplets all have the same diameter at any given time and that the total liquid surface area is conserved (i.e., the Sauter mean diameter is utilized). Previously, the droplet diameter has been read in as a function of piston travel.[2,3] However, in this case, the difference in piston travel is as important as the absolute travel. Thus, an option was added to enter the droplet diameter as a function of chamber pressure.

The liquid accumulation and the droplet mean diameter can also be derived from the inverse code. However, approximations must be made, and the results are even less accurate than the discharge coefficient derivations. Figure 16 shows the derived liquid accumulation and Figure 17 the corresponding droplet mean diameter (solid lines). Figure 17 also shows the profile finally chosen for the droplet model (dotted line), and Figure 16 shows the corresponding accumulation predicted by the gun code. The reasons that the profile derived by the inverse code was not adequate are discussed below. The droplet profile was in practice chosen by trial and error until the code results matched the chamber pressure profile. The droplet diameters were constrained to decrease over the course of the firing cycle. It proved very difficult to match the larger pressure profile F30 but straightforward to match the lower pressure profile F120. For this reason, the shot-start value of 24 MPa associated with the lower experimental chamber pressure was used in the model. The projectile resistance pressure was increased from 2.5 MPa to 3.5 MPa to obtain the experimental muzzle velocity of 776 m/s exactly. The appendix shows the input job stream for the droplet model and the summary output page. Table 2 shows the particular droplet profile used.

Figures 18 through 22 compare the final model with the experimental values. The model follows the lower pressure curve F120 very closely up to peak pressure. At this point, the experimental pressure drops much more rapidly than does the model. Even if combustion is shut off, the model cannot produce this rapid pressure drop. However, GE has reported problems with pressure gauges. After peak pressure, if the gauges become hot, the measured pressure will be low. This may account for the rapid pressure drop recorded at the gauge F120. The liquid pressure is close to the lower experimental pressures. The calculated damper pressure shows rough agreement with experiment. The flow out of the damper is probably more complicated than steady-state Bernoulli flow with a constant discharge coefficient. However, the piston travels are now very accurate, which is what is required to match the gun performance. The projectile travel matches the available experimental data well.
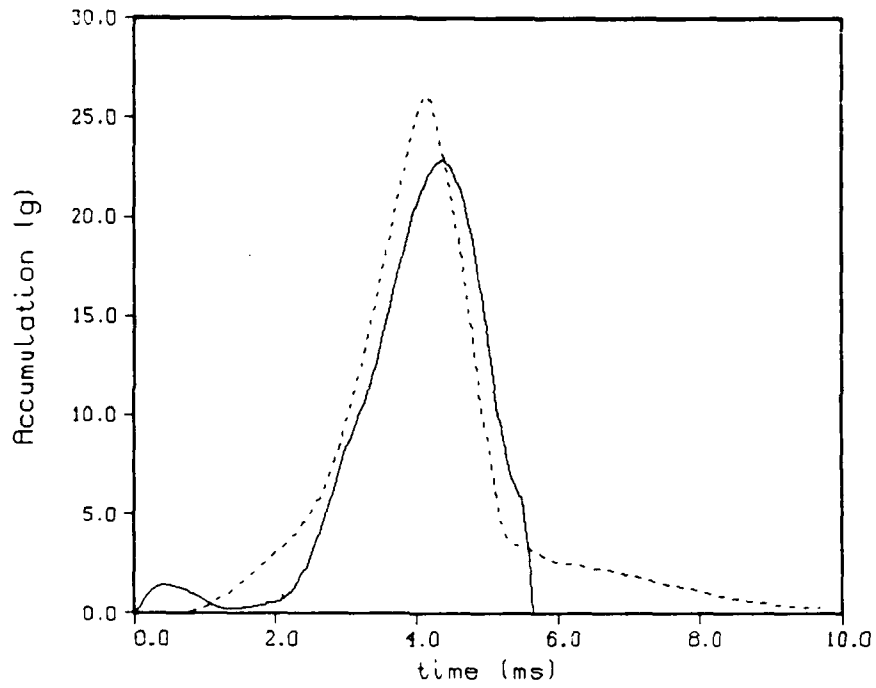
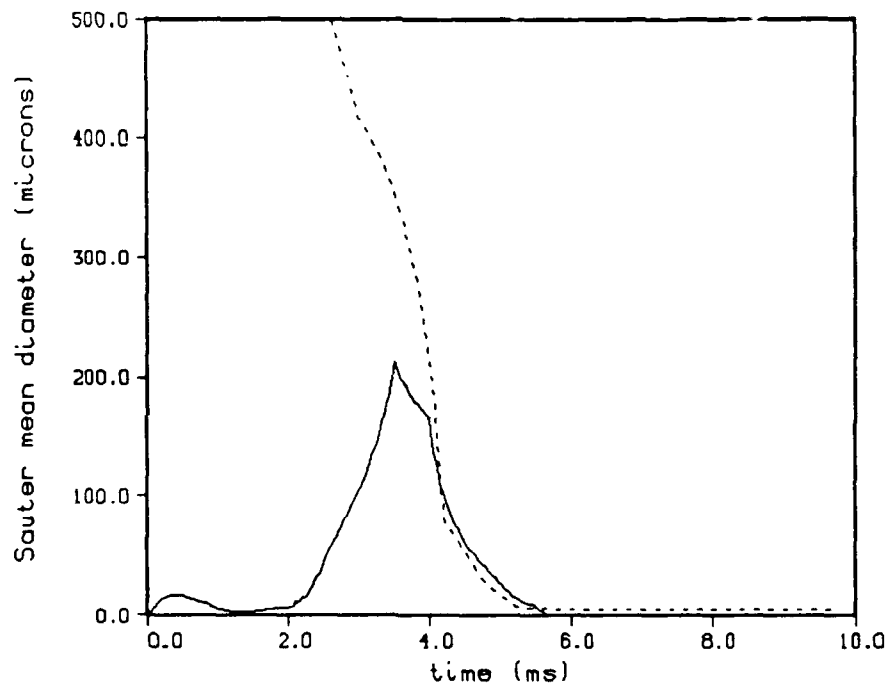Figure 16. Liquid Accumulation - Round 51 - From Inverse Code (line). Model With Droplet Burning (dot).

Figure 17. Sauter Mean Diameter - Round 51 - From Inverse Code (line). Model With Droplet Burning (dot).

26

TABLE 2. Round 51 Mean Droplet Diameter Profile.

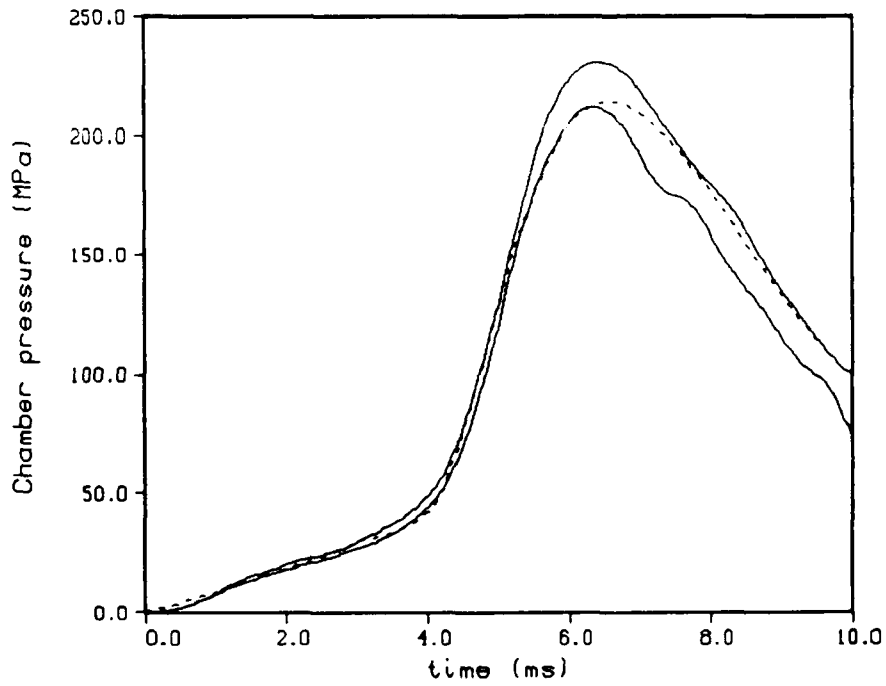| Chamber pressure, MPa	Droplet diameter, μ
0	500
25	500
50	80
100	30
150	8
200	5

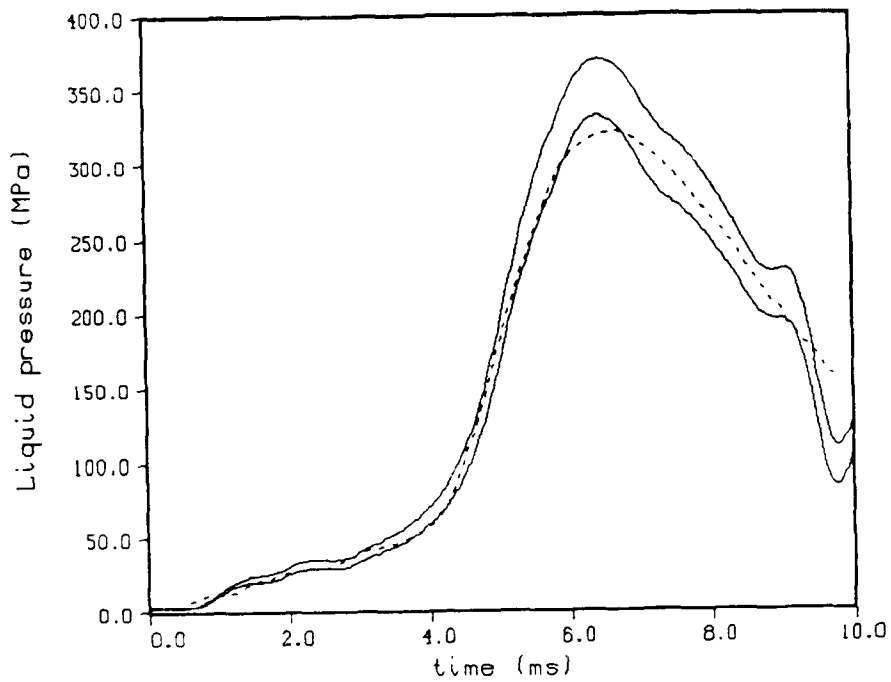Figure 18. Chamber Pressure - Round 51 (line). Model With Droplet Burning (dot).

27

Figure 19. Liquid Pressure - Round 51 (line). Model With Droplet Burning (dot).
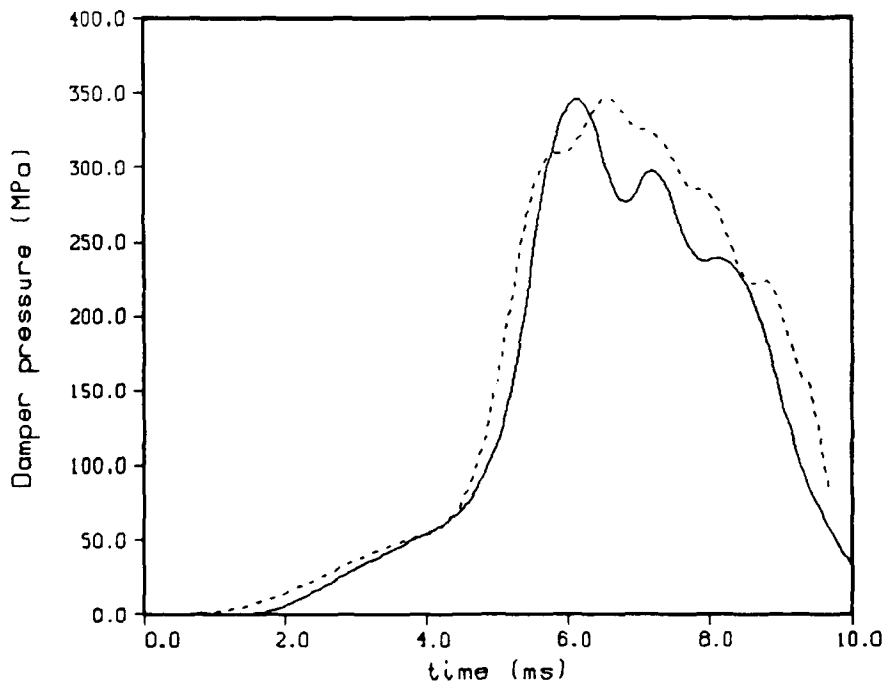

Figure 20. Damper Pressure - Round 51 (line). Model With Droplet Burning (dot).
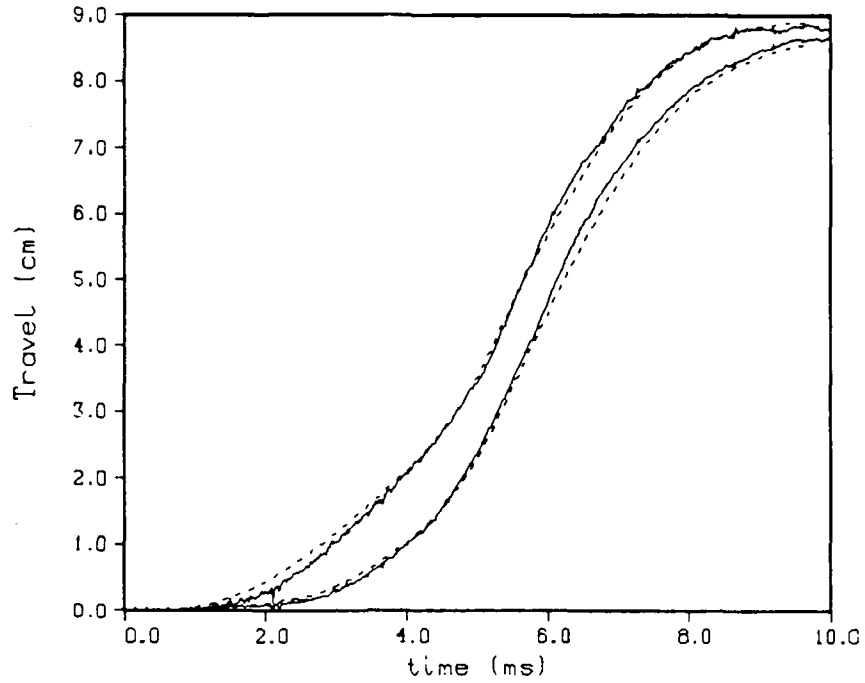
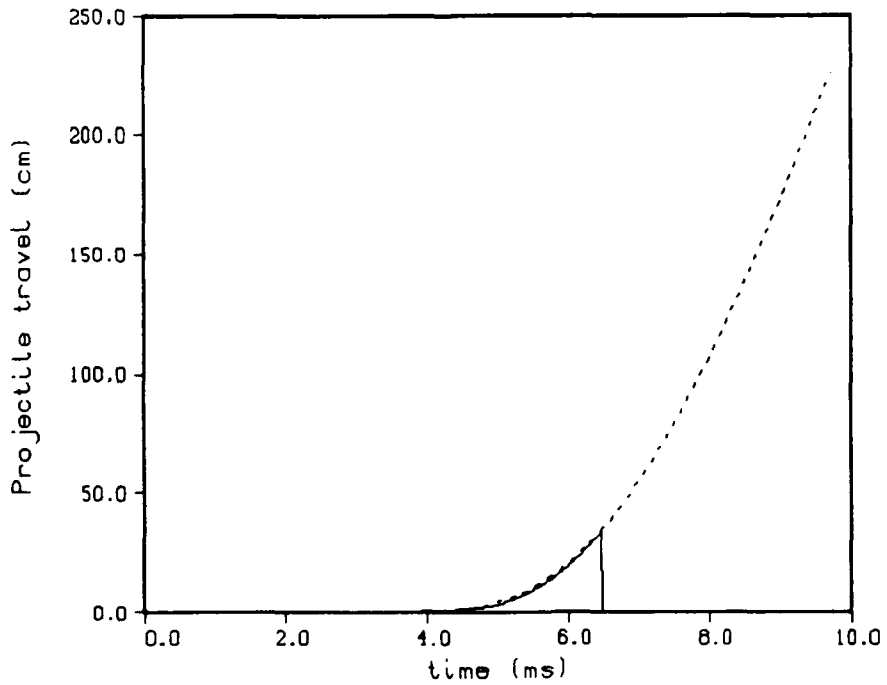Figure 21. Piston Travels - Round 51 (line). Model With Droplet Burning (dot).

Figure 22. Projectile Travel - Round 51 (line). Model With Droplet Burning (dot).

Now suppose that our droplet profile is taken directly from the inverse code calculations (Figure 17, solid line). The resulting chamber pressure profile is shown in Figure 23. The model pressure increases more rapidly than do the experimental curves.

However, this does not necessarily indicate an error in the inverse code. In fact, at early times, the liquid propellant sheet is very thin, and one would expect small droplets. There are other effects, as well, that could cause a delay in the pressure rise.

Consider instead the effect of varying the discharge coefficient out of the reservoir. Since the liquid is prepressurized, at the start of the firing cycle the liquid pressure is 35 times higher than the chamber pressure. This is far from steady-state conditions. The flow could easily be less efficient than predicted by the steady-state Bernoulli equation. So the discharge coefficient was set to 0.5 over the first 0.3 cm of outer piston travel and then increased to 0.95 after 0.5 cm of piston travel. Figure 24 shows the result. The chamber pressure now shows very good agreement with experiment.

Another possibility concerns the primer model. The primer is assumed to inject gas at a constant rate over the first 3.0 ms. During this time, the primer injects almost as much mass as does the reservoir. Previously, it was assumed that 50 percent of the energy of the primer was lost. If 60 percent is assumed lost instead, this will delay the chamber pressure rise substantially. Figure 25 shows the chamber pressure for this primer model, using an inverse droplet model and a constant discharge coefficient of 0.95. The agreement is not as good as that in Figure 24 but is much improved over the original inverse model in Figure 23.

Due to the sensitivity of the chamber pressure at early times to small changes in energy release, we are unable to determine the source of the discrepancy between model and experiment. However, it is felt that the most likely explanation is in fact a smaller discharge coefficient. Figure 21 shows that the model piston travels are slightly faster than those of the experimental values. For best agreement, the model piston motion should be slowed down slightly. This can be done most easily by lowering the discharge coefficient. However, this could also be done indirectly by changing the damper model.

Because of these uncertainties, our original droplet model will be retained for the present as the simplest approximation to the data. It is noted that the actual droplet sizes used in the model may have no physical significance. However, we are attempting to address this issue in ongoing research efforts.
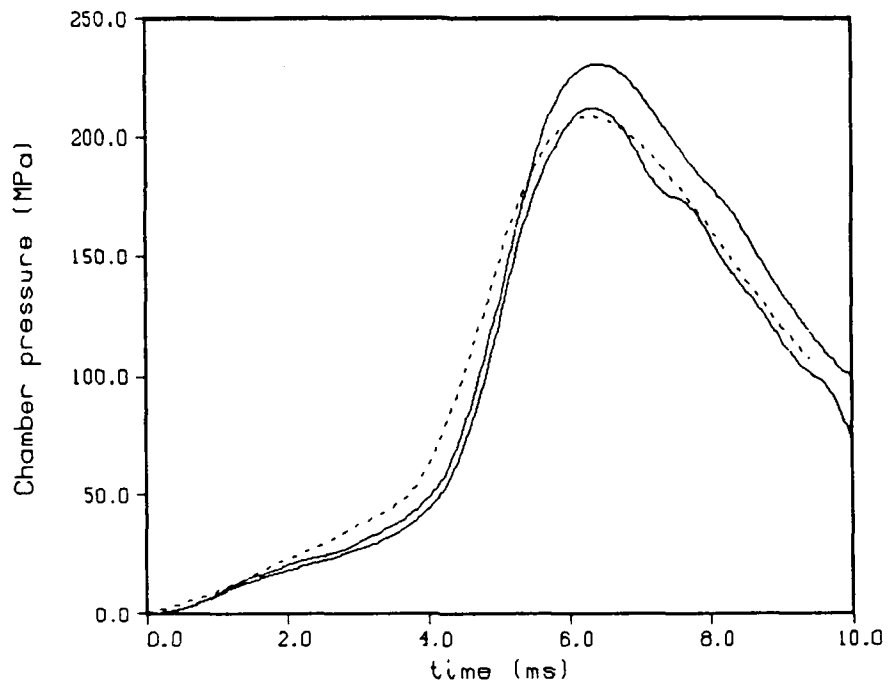
Figure 23. Chamber Pressure - Round 51 (line). Model With Inverse Code Droplet Profile (dot).
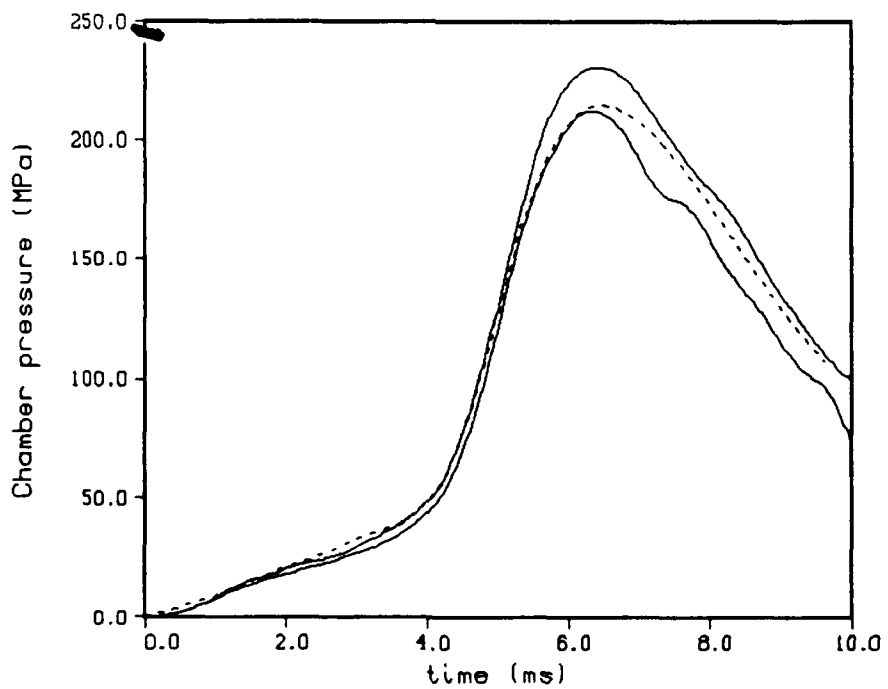

Figure 24. Chamber Pressure - Round 51 (line). Model With Inverse Code Droplet Profile (dot). Modified Discharge Coefficient.
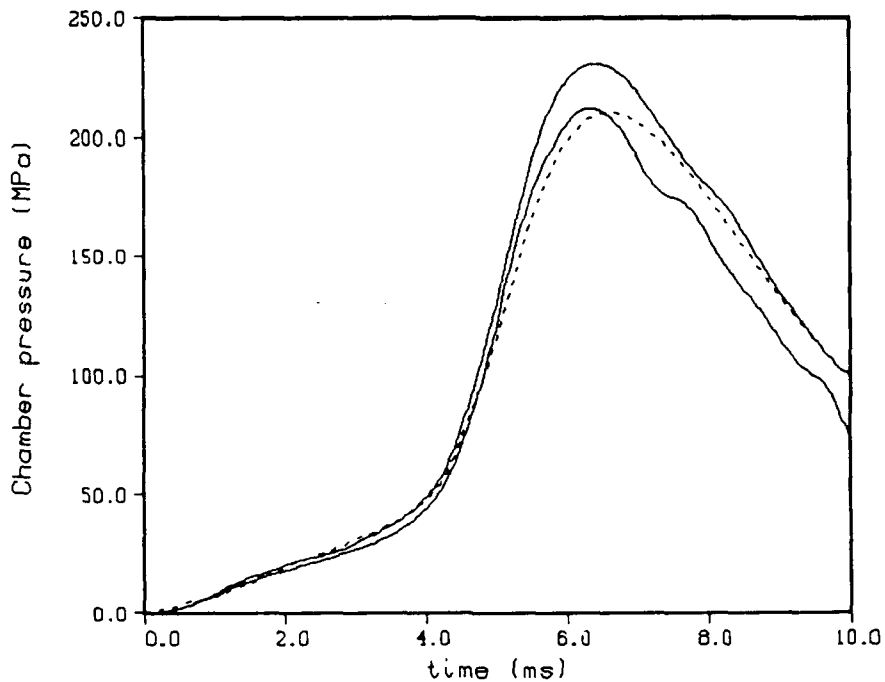
Figure 25. Chamber Pressure - Round 51 (line). Model With Inverse Code Droplet Profile (dot). Modified Primer Heat Loss.

8. GE 30 MM GUN FIXTURE - OTHER CONFIGURATIONS

Since a match was obtained with experimental data in the repeatability series (medium charge, 230 cc liquid propellant) it was of interest to determine if the model could be used in a predictive mode for the two other configurations of liquid volume and initial combustion chamber volume. Shots 12 to 23 were made with a short propellant charge (94 cc liquid charge and 1.41 inch stroke) with two different initial chamber volumes (280 cc and 747 cc). The fixture has not been fired with a full charge. The changes in gun dimensions were made in the code. The discharge coefficients and the droplet distribution were left unchanged. After shot 27, the engraving band on the projectile was redesigned, causing a change in shot start pressure. The shot start pressures used are those recorded by GE from the radar data.[4]

Shots 12 through 17 were made with the same configuration. The mean muzzle velocity was 622 m/s with a standard deviation of 0.72 percent. Table 3 shows the differences between this series of shots and the medium charge series. There is much less liquid propellant being injected into a smaller chamber. The primer mass is reduced because of the smaller initial chamber volume. The change in the engraving band caused a higher shot start pressure. The damper volume was smaller. A different bolt was attached to the back of the control rod, creating a different damper vent area profile (see Figure 26).

32

TABLE 3. Differences Between Shot 51 and Shot 15.

	Piston stroke, in	Initial liquid volume, cc	Initial chamber volume, cc	Shot start pressure, MPa	Premier mass, g	Initial damper volume, cc
Shot 51	3.5	232.9	500.0	24.0	29.0	57.1
Shot 15	1.41	93.8	280.0	33.3	15.5	28.6

Note: Differences in damper vent table are shown in Figure 26.
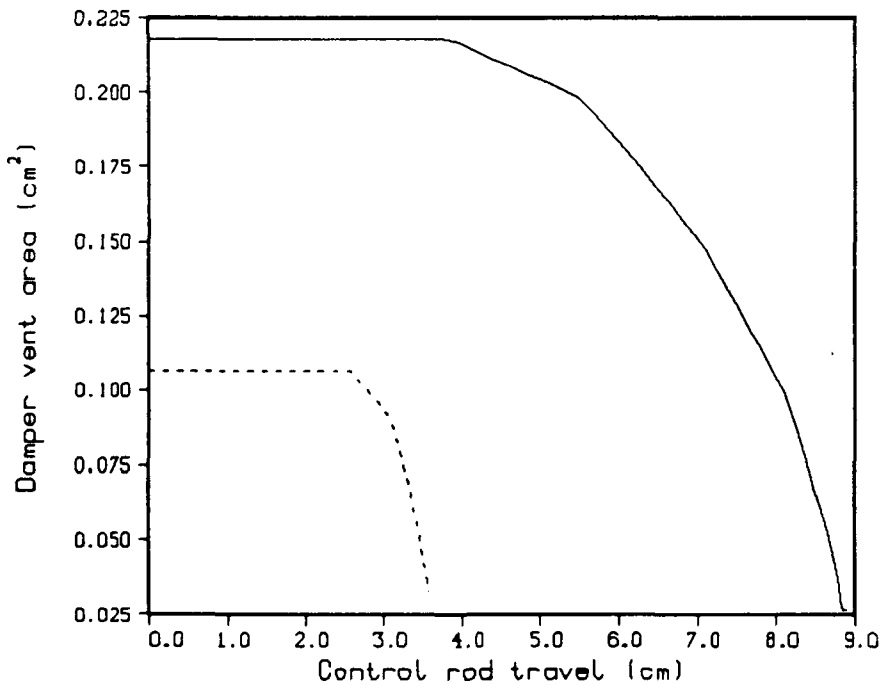

Figure 26. Damper Vent Area vs. Control Rod Travel. Round 51 (line). Round 15 (dot).

A second series of shots (see Table 4) was made with a much larger chamber (shots 18-23). The stroke was intended to be the same, but in practice the transducer block was pushed forward, causing a slightly shorter stroke. The muzzle velocity was 547 m/s with a standard deviation of 1.17 percent.

These two cases were simulated using the model described above. Table 5 shows the resulting muzzle velocities. The agreement between the experiment and the model is very good.

Unfortunately, there is not very good agreement with the pressure profiles (see Figures 27 and 28). In particular, the experiments show an earlier pressure rise than do the model profiles. There is less accumulation in the two short charge cases than there is in the medium charge series. This can be explained in terms of the new damper profile. The damper vent area is very small at the start of the firing cycle. As a result, the control rod moves slowly, and the reservoir vent area also stays small (see Figure 29). Since the liquid is now injected in a thinner sheet, it breaks up and burns more efficiently.

An earlier presentation was made of the above results.[12] There have been several minor changes in the model since that time. The main difference was in the attempt to predict the performance of the short charge firings. The round 51 shot start was used, instead of the shot start appropriate to the earlier engraving band. The predicted muzzle velocities and maximum chamber pressures were both smaller. This caused better agreement with the experimental chamber pressure and worse agreement with the experimental muzzle velocities.

The shot start pressure is an important parameter. If the shot start pressure is increased, both the maximum chamber pressure and the muzzle velocity will increase. In this case, changes in the shot start pressure can cause good agreement in maximum chamber pressure or in muzzle velocity, but not in both.

9. FURTHER MODELING - SHORT CHARGE

The parameters derived in the baseline study are adequate for predicting the performance of the gun with the short charge. However, it was felt that differences between the values used in the predictive mode and the values required to more accurately represent the experimental data may better illuminate the physics. Thus, new values for the experimental parameters are derived for the short charge firings.

TABLE 4. Differences Between Shot 15 and Shot 22.

	Piston stroke, in	Initial liquid volume, cc	Initial chamber volume, cc	Shot start pressure, MPa	Primer mass, g
Shot 15	1.41	93.8	280.0	33.3	15.5
Shot 21	1.36	90.4	747.0	31.3	36.0

TABLE 5. Muzzle Velocities.

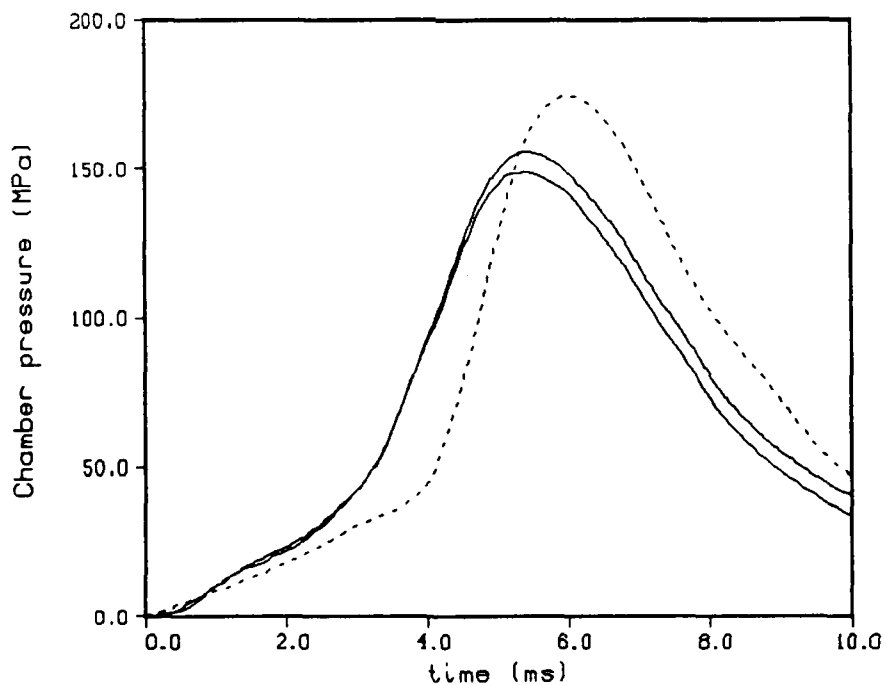| Round	Experimental	Model	Percent Difference
51	776	776	0.0
15	622	624	0.3
22	547	543	-0.7

Figure 27. Chamber Pressure - Round 15 (line). Model With Round 51 Droplet Profile (dot).
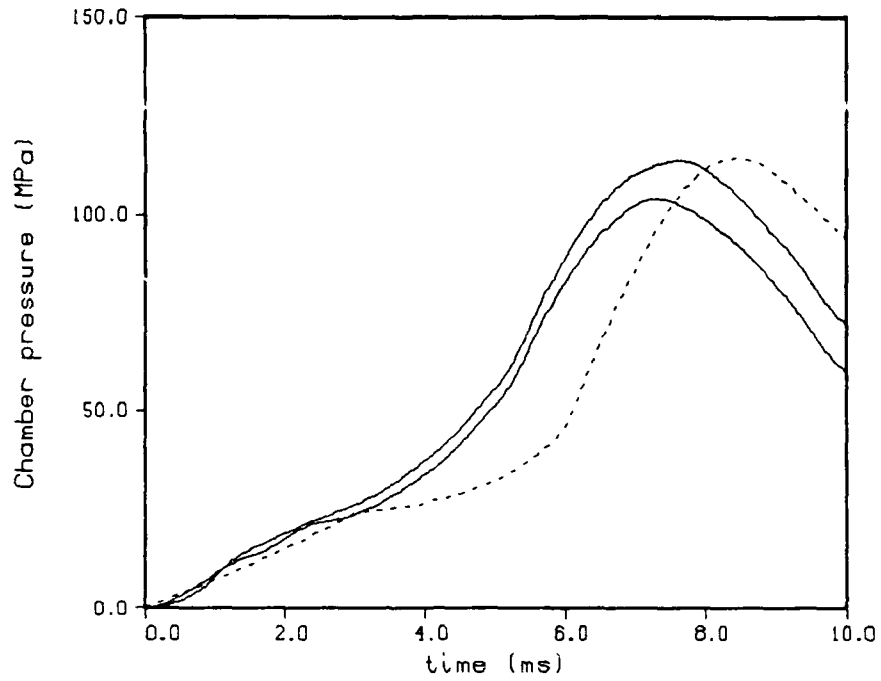
35

Figure 28. Chamber Pressure - Round 22 (line). Model With Round 51 Droplet Profile (dot).
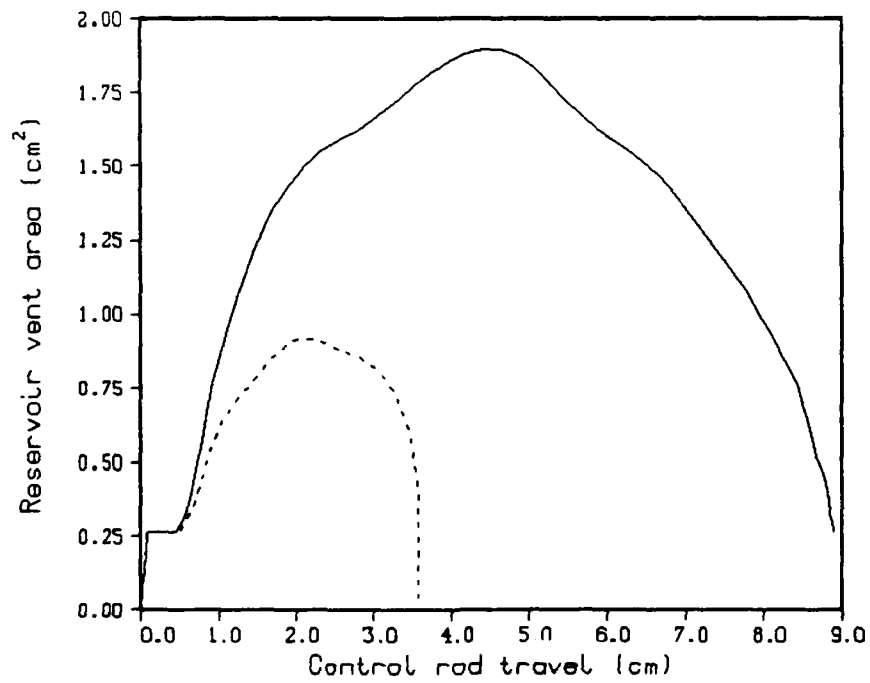

Figure 29. Reservoir Vent Area vs. Control Rod Travel. Round 51 (line). Round 15 (dot).

Typically the discharge coefficients are rederived first, since neither the reservoir nor the damper discharge coefficients can be measured directly. Unfortunately, the piston travels for the early shots were recorded using a double-headed optron later found to be very inaccurate. Thus, the recorded piston travels are not useful, and discharge coefficients cannot be extracted from the data. Instead, only the droplet diameter profile is readjusted (Table 6). This is varied to obtain a reasonable agreement for the Round 15 chamber pressure. Figures 30 and 31 show the results. The agreement in pressure is quite good. The same droplet profile is used for the large chamber tests (Figures 32 and 33). The agreement is still good. The same parameters can be used for both the short charge sets of tests. However, the corresponding muzzle velocities are in poorer agreement with experimental data, as shown in Table 7. The cause of the discrepancy is not known, but the most likely explanation is a change in the discharge coefficient for the flow out of the damper.

10. DISCUSSION

One long-term goal is to be able to predict the performance of a gun design. In Section 7, excellent agreement was demonstrated between the model and the experimental data. This is reassuring, considering the simplicity of the physics in the model. However, several model parameters were derived from the experimental data. In this section, we will discuss the uncertainties in the derived parameters and the prospects for using this data to model new gun designs.

The primary difficulty in deriving parameters is the error in the chamber pressure measurements. There are calibration problems with the gauges, as well as gauge drift due to heating after peak pressure. Since all of the derived parameters depend heavily on the chamber pressure, this is a major potential source of uncertainty in the analysis.

The discharge coefficient out of the reservoir was set at a constant value of 0.95. This is reasonable for high-speed flow with no major losses. Preliminary work on other VIC guns indicates that this is a very good approximation for the larger caliber guns as well as for the 30 mm fixture. If the piston is redesigned with sharper corners, such that flow separation becomes more likely, this approximation must be reassessed. We also note that analyses presented in this paper indicate that the discharge coefficient is smaller than 0.95 at very early times in the ballistic cycle.

37

TABLE 6. Round 15 Mean Droplet Diameter Profile.

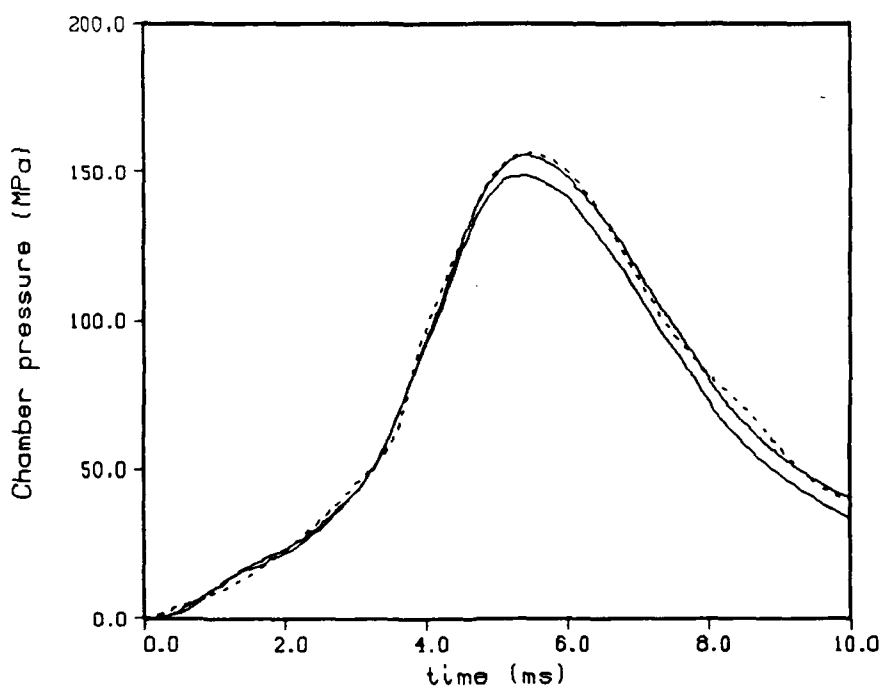| Chamber pressure, MPa	Droplet diameter, μ
0	75
50	75
75	10
125	10
150	1

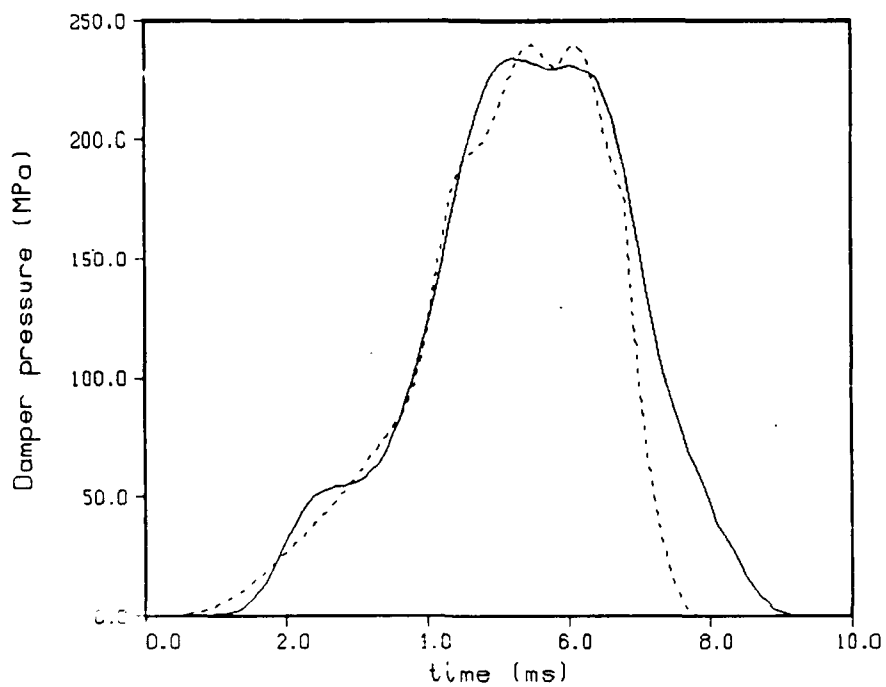Figure 30. Chamber Pressure - Round 15 (line). Model With Droplet Burning (dot).

Figure 31. Damper Pressure - Round 15 (line). Model With Droplet Burning (dot).
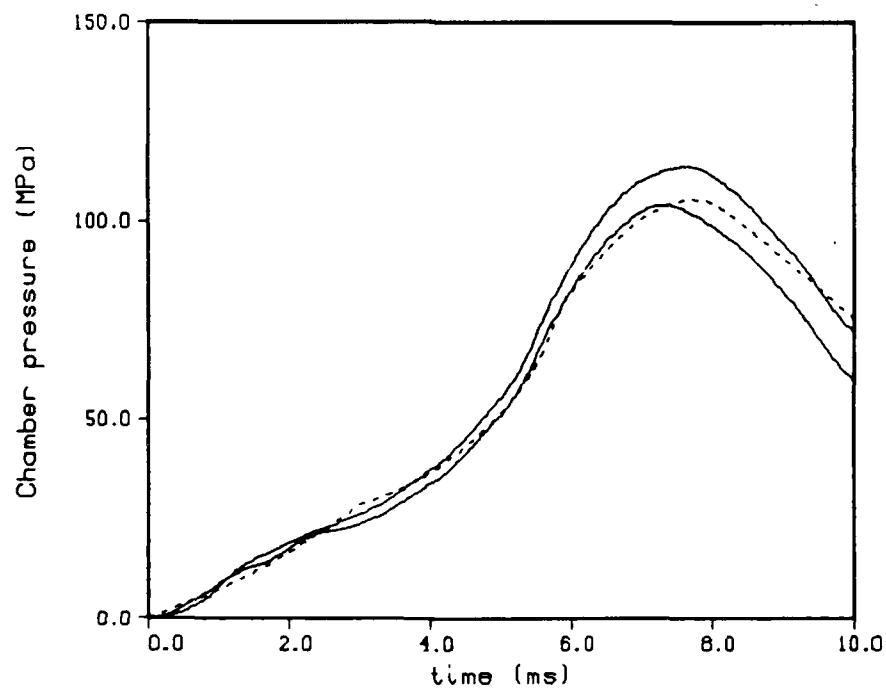

Figure 32. Chamber Pressure - Round 22 (line). Model With Round 15 Droplet Profile (dot).
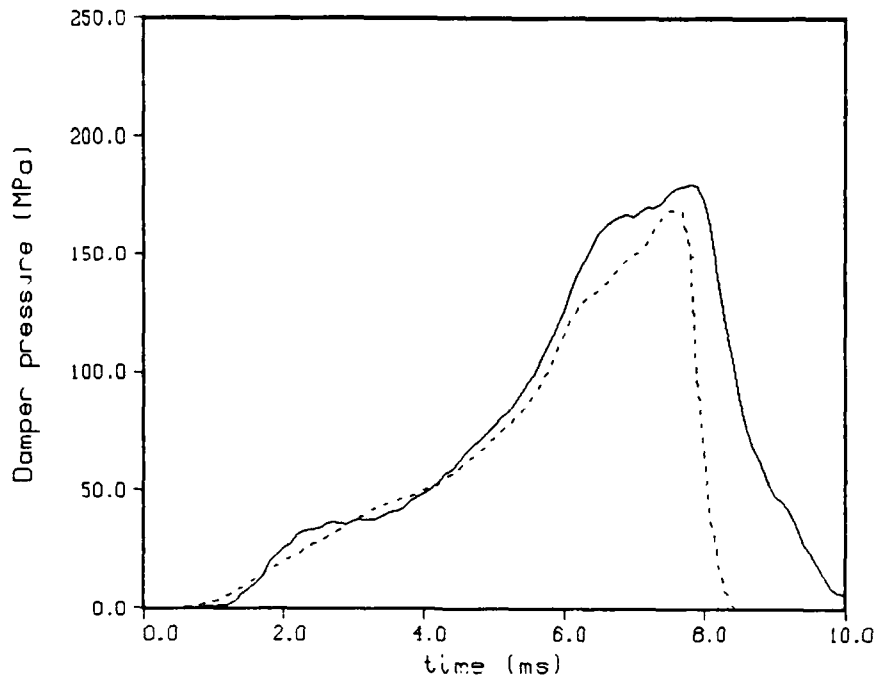
39

Figure 33. Damper Pressure - Round 22 (line). Model With Round 15 Droplet Profile (dot).

TABLE 7. Comparison of Experimental and Simulated Muzzle Velocities
with Improved Droplet Diameter Profile.

Round	Experimental	Model	Percent Difference
15	622	610	-1.9
22	547	535	-2.2

The discharge coefficient out of the damper is more complicated. Flow here is through a smaller vent with a sharp corner across a larger pressure difference. Assuming a constant discharge coefficient is a reasonable approximation, but the flow is actually more complicated, especially near the end of the stroke. At present, we have not developed a method of estimating the discharge coefficient. It must be derived from experimental data for a particular damper design.

The parameters for the primer model are generated by analyzing data from a water shot, in which water, rather than liquid propellant, is initially placed in the reservoir. However, it is not really known how the early combustion of the propellant will effect the primer injection. A more detailed primer injection model may be required.

The engraving band on the projectile was redesigned partially to obtain a more reproducible shot start pressure. Nevertheless, GE reported shot start pressures between 21.3 MPa and 26.5 MPa for shots 28 through 51. It is unknown how much of this variation is due to actual changes in the shot start pressure and how much is due to errors in the chamber pressure measurements. Data must be obtained for a given projectile design to obtain an estimate of the shot start pressure.

The droplet model is the most complicated parameter. Since the mean droplet diameter is allowed to vary with pressure, this can compensate for some errors in the other parameters. However, the droplet profile does offer only limited leverage. In earlier simulations, when incorrect values for some of the physical parameters (i.e., design parameters) were used, it proved impossible to match the chamber pressure by any adjustments in the droplet profile.

We plan to try to correlate the droplet diameter with other physical parameters in the code (i.e., gas density, jet velocity, injection gap) to try to obtain a predictive model for jet breakup and droplet formation. This requires a knowledge of the sensitivity of the droplet profile to changes in other parameters. We have already seen that the early droplet diameter depends heavily on the values chosen for the reservoir discharge coefficient and the primer injection model.

In order to assess the sensitivity of droplet diameter to other derived parameters, a simple study was performed. Our derived parameters were varied one at a time, and the droplet profile was rederived to obtain close agreement with the original chamber pressure curve and the experimental muzzle velocity. The five resulting simulations are:

A. The baseline round 51 droplet model.
B. The reservoir discharge coefficient was changed from 0.95 to 0.90.

C. The damper discharge coefficient was changed from 0.70 to 0.80.

D. The shot start pressure was changed from 24 MPa to 30 MPa.

E. The primer injection time was changed from 3.0 ms to 4.0 ms.

Table 8 shows the resulting droplet profiles. Predicted muzzle velocities are also given in this table. It proved impossible to match the muzzle velocity in all cases while remaining close to the desired chamber pressure, leaving all other input values fixed. Figure 34 shows the chamber pressure profiles for the five cases.

The change in the reservoir discharge coefficient had the least effect. However, the droplet diameter had to be made smaller at high pressures to obtain the same maximum pressure and muzzle velocity. Since the liquid was injected more slowly, more efficient combustion was required.

The change in the damper discharge coefficient caused a major change. If the early pressure curve was matched, it proved impossible to stop the pressure rise at the proper level. Even with much larger droplets, the predicted muzzle velocity was much too high.

The change in shot start was less dramatic but did require a larger drop size. If the proper peak pressure was obtained, the predicted muzzle velocity increased slightly.

Changing the primer injection model had the most dramatic result. It proved impossible to track even the shape of the pressure curve at the point of rapid pressure rise near 4.0 ms. Also, the desired muzzle velocity could not be obtained.

These results are somewhat mixed. The good agreement obtained in the earlier sections does not appear to be simple curve fitting. The chamber pressure profile and muzzle velocity can only be reproduced for a limited set of parameter values.

On the other hand, the droplet profile derived is not unique. Fairly small changes in the other parameters can lead to large changes in the droplet diameter profile. This must be kept in mind when looking for correlations for the droplet sizes.

42

TABLE 8. Sensitivity of the Droplet Profile to the Other Derived Parameters.

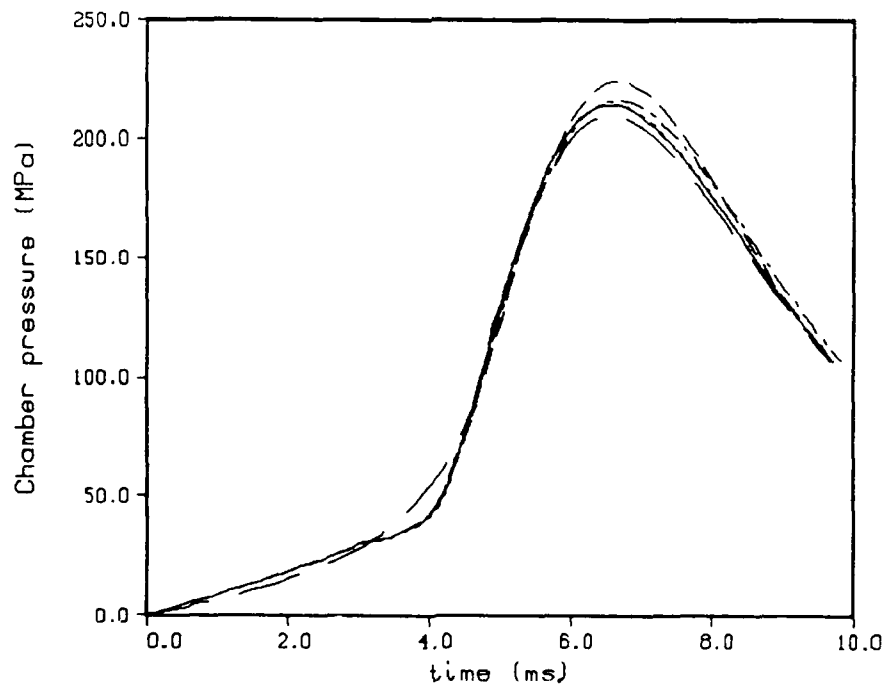| Pressure, MPa	A	B	C	D	E
0	500	500	500	500	100
25	500	500	500	500	100
50	80	75	100	80	100
100	30	25	50	40	20
150	8	5	25	20	5
200	5	1	25	20	1
v_m	776	776	789	780	771

Figure 34. Baseline Round 51 Droplet Model (line). C_D - Reservoir = 0.90 (dot). C_D - Damper = 0.80 (dash). Shot Start = 30 MPa (dot-dash). Injection Time = 4.0 ms. (long dash).

43

11. CONCLUSIONS

A model has been developed for the Concept VIC regenerative liquid propellant gun that incorporates the major features of the gun in a lumped parameter form. Most of the needed parameters are physical dimensions and properties that can be chosen without reference to experimental data. However, parameters that must be benchmarked from a study of the data are the discharge coefficient out of the reservoir, the discharge coefficient out of the damper, the shot start pressure, the primer injection time scale and heat loss factor, and the droplet diameter profile. A constant discharge coefficient of 0.95 for the reservoir, and 0.70 for the damper, works well for all of the 30 mm firings studied (assuming steady-state Bernoulli flow). The droplet diameter profile should be changed, depending upon the damper profile. The short charge length firings have a much smaller damper exit area leading to a smaller reservoir exit area, which strongly affects the liquid accumulation.

The model is able to match experimental data from the 30 mm Concept VIC RLPG using reasonable values for parameters that cannot be measured. Using the model in a predictive mode with parameters determined from a benchmark case, configurations in which the charge size and initial combustion chamber volume have been substantially changed are modeled reasonably well. The performance of the model can be enhanced by taking into account changes in the liquid propellant sheet thickness in the droplet diameter profile.

12. REFERENCES

1. "Regenerative Liquid Propellant Gun Technology Transition Criteria," Meeting of LP management detailing transition criteria from BRL to ARDEC. Picatinny Arsenal, NJ, November 1988.

2. Coffee, T. P. "A Lumped Parameter Code for Regenerative Liquid Propellant Guns," BRL-TR-2703. U.S. Army Ballistic Research Laboratory, Aberdeen Proving Ground, MD, December 1985.

3. Coffee, T. P. "An Updated Lumped Parameter Code for Regenerative Liquid Propellant In-Line Guns," BRL-TR-2974. U.S. Army Ballistic Research Laboratory, Aberdeen Proving Ground, MD, December 1988.

4. Cunninghan, C. R., Walter, B. R., and Lavin, K. "Regenerative Liquid Propellant Gun Test Results for 30 mm Concept VIC." Paper presented at 25th JANNAF Combustion Meeting, Huntsville, AL, October 1988.

5. Coffee, T. P. "The Analysis of Experimental Measurements on Liquid Regenerative Guns," BRL-TR-2731. U.S. Army Ballistic Research Laboratory, Aberdeen Proving Ground, MD, May 1986.

6. Coffee, T. P. "Injection Processes in Liquid Regenerative Propellant Guns," BRL-TR-2846. U.S. Army Ballistic Research Laboratory, Aberdeen Proving Ground, MD, August 1987.

7. Bulman, M. "Regenerative Liquid Propellant Tank Guns," Preliminary Status Report, General Electric, Pittsfield, MA, August 1987.

8. Coffee, T. P. "One-Dimensional Modeling of Liquid Injection in a Regenerative Propellant Gun," BRL-TR-2897. U.S. Army Ballistic Research Laboratory, Aberdeen Proving Ground, MD, March 1988.

9. Baer, P. "Practical Interior Ballistic Analysis of Guns," in Krier, H. and Summerfield, M., Interior Ballistics of Guns, Volume 66: Progress in Astronautics and Aeronautics, New York University, New York, 1979.

10. McBratney, W. F. "Windowed Chamber Investigation of the Burning Rate of Liquid Monopropellants for Guns," BRL-MR-03018. U.S. Army Ballistic Research Laboratory, Aberdeen Proving Ground, MD, April 1980.

11. McBratney, W. F. "Burning Rate Data, LPG 1845," BRL-MR-03128. U.S. Army Ballistic Research Laboratory, Aberdeen Proving Ground, MD, August 1981.

12. Wren, G. P. "Transition Criteria: Modeling of 30 mm VIC Regenerative Liquid Propellant Guns." Paper presented at the Liquid Propellant Quarterly Meeting, Picatinny Arsenal, December 1988.

APPENDIX:
INPUT PARAMETERS FOR BASELINE MODEL

Intentionally left blank.

Below is a listing of the job stream for the baseline model (Round 51 - droplet burning). The numbers and labels at the left are read in by the code. The comments at the right are for identification by the user and do not effect the actual code. Following is the summary sheet from the output file. A description of the input and a brief description of the source for the input variables are given first.

The first line is merely a label. It lists the filename of the input job stream and a brief description of the problem.

The initial offset of the projectile and the total distance traveled by the projectile before muzzle exit are given. The diameter of the gun tube is given. The projectile and piston weights are entered (measured by GE). The actual projectile weight does vary a few grams from shot to shot. This variation is not important, and the nominal value is used.

The initial volume of the liquid reservoir is given. GE reports a volume of 230 cc and a piston stroke of 8.89 cm. The nominal liquid volume is raised slightly to match the piston stroke. The initial gas volume is as reported by GE. The initial areas of the reservoir (including control rod) and chamber are derived from the engineering drawings.

The VENT4 option is chosen (VIC gun). The control rod radius versus relative piston motion is gotten from the drawings. The zero point is where the outer piston and control rod first fit together. The positive direction is to the left (direction of the piston stroke). In this case only the parts of the control rod to the right (negative direction) are relevant, since the outer piston cannot move to the left with respect to the control rod. The area of the hole in the outer piston is computed from the engineering drawings. There is no grease dyke on this piston.

The piston resistance is set to zero, since this is not usually large enough to be important. The discharge coefficient into the chamber is set at a constant 0.95 (see section 7). The discharge coefficient into the gun tube is set equal to one (no losses).

The flow into the chamber is modeled as steady state Bernoulli flow (FLUX1). There is only one vent hole. The piston thickness is irrelevant for this option. The flow into the gun tube is steady state isentropic flow, assuming the more complicated gun tube pressure gradient model (FLUX2).

The shot start is taken as 24 MPa. The shot start pressure is applied over a distance of 0.468 in = 1.19 cm (one and a half times the length of the engraving band) and then rapidly dies down. After shot start the resistance pressure is taken as 3.5 MPa.

Next the physical properties of the propellant HAN1846 are given.

The liquid is pre-pressurized to 3.5 MPa. The initial chamber pressure is one atmosphere.

The droplet diameter is read in as a function of chamber pressure (DROP4). The burning rate is read as a two part function. There is some evidence that there is a break in the slope of the burning rate just under 100 MPa. However, since the rate at higher than 100 MPa is not known, the rate that was measured for lower pressures is used. The code does allow a two part burning rate to be entered. The droplet diameter table has been chosen to match the chamber pressure. However, the final minimum droplet diameter was chosen to match the experimental muzzle velocity.

The primer is injected in the form of hot gas (PRIM3). The actual primer mass is 29 g. The primer has been adjusted so that the chamber pressure will increase at a rate of 7 MPa/ms for about 3 ms. The injection time is taken as 3.0 ms. The default heat loss of 50 percent is used. This gives about the right chamber pressure if the gun code is run without combustion (very large droplets).

The default models for the heat loss to the gun tube and the air shock are used. Heat loss to the combustion chamber walls is ignored.

The most complicated Lagrange model (TUBE4) is chosen. The model will take into account the rarefaction wave after burnout of the propellant.

The damper or buffer model is chosen (BUFF2). These areas of the damper side of the control rod and the hole in the block are from the engineering drawings. The area of the 1/32 in diameter hole drilled into the damper is taken into account. The discharge coefficient is set equal to 0.70 (see section 7). The initial volume is estimated from the drawings. The damper is originally pressurized to 0.34 MPa to reduce ullage. The damper fluid is water, which has a density of 1.0 g/cc. The bulk modulus and the derivative of the bulk modulus with respect to pressure were derived from data in a report by Constantino.

50

The vent area is given as a function of control rod travel. The bolt on the back of the control rod has been cut to make this vent. Two flat surfaces are cut on opposite sides of the bolt. The engineering drawings give the depth of the cut versus the rod travel. From this information the actual vent area was computed.

The code will print out results every 0.1 ms (TINC). Because the code must often change the time step, it is more efficient to restrict the maximum time step (HTOP). The error controls EPS and SREC are given typical values.

The integration method flag MF is set to 22 (backwards differentiation formulas with an internally computed Jacobian). KWRITE is set to zero to eliminate diagnostic messages. A time limit of TMAX is set. If the code takes longer than TMAX seconds to execute, the code will stop gracefully and write the usual summary pages.

The code is only to be integrated once (REP1) and the chamber pressure will be computed normally (CHAM1).

```
dt51 - VIC - medium charge - Drop - cd=0.95 - cd5=0.70
   0.0         226.         offset    proj travel
   3.0                      gun tube diameter
 682.                       proj weight
2540.                       piston weight
 232.9        500.          v1    v3
  33.781       45.513       a1    a3
vent4                       moving central bolt
  23                            bolt radius versus piston travel
    -2.4308     1.2497
    -0.5588     1.6129
    -0.5309     1.6180
    -0.5055     1.6231
    -0.4801     1.6256
    -0.4547     1.6307
    -0.4039     1.6332
    -0.3531     1.6383
    -0.3023     1.6383
    -0.0508     1.6383
     0.0000     1.6637
     0.3912     1.8593
     0.4039     1.8593
     0.4293     1.7374
     0.4547     1.6915
     0.4801     1.6586
     0.5055     1.6332
     0.5309     1.6129
     0.5563     1.5951
     0.6071     1.5723
     0.6579     1.5596
     0.7087     1.5545
    38.1000     1.5545
   8.696      .0            ahole     agres
    1530.                   rodwt
pis1                        piston resistance
  2
    0.0       0.0
    1.0       0.0
dis1                        dis. coeff. versus piston travel
  2
    0.0       .95
    1.0       .95
dis1                        dis. coeff. vs. proj travel - tube
  2
    0.0     1.0
  226.00    1.0
flux1                       steady state mass flux formulation
  1           1.0             nvo    pth
flux2                       isentropic flow into tube

proj1                       proj resistance
  4
    0.0         24.
```

52

```
     1.19          24.
     1.20           3.5
   226.00           3.5
     1.43   5350.0   9.11     rh0    k1    k2
  4035.5        1.2226        energy    gamma
    66.9        .04988        surface tension    kinematic viscosity
    22.848      .677          mol wt gas      covolume
     3.5        0.1           p1    p3
  drop4                       droplets
     0.01     95.2590         ddr       pbr
     1.64       .103          adr1      bdr1
     1.64       .103          adr1      bdr1
     7
     0.0          .0500
    25.0          .0500
    50.0          .0080
   100.0          .0030
   150.0          .0008
   200.0          .0005
  1000.0          .0005
  prim3                       inject hot gas
    29.0     0.003      0.5      primer mass    injection time    heat loss
  heat1                       no heat loss to chamber walls
  heat2                       heat loss to gun tube walls
   300.0      1.0             tube temp    fudge factor
  shock2                      air shock
     0.1      300.              airp    airt
     1.4      28.84             airgam airmw
  tube4                       unsteady lagrange distribution
  burn
  buff2                       buffer - water
     7.591     2.526   .0049   apis   ahole  acir
      .70                      cd5
    57.1                       v5
      .34         .34          p5     pout5
     1.0      2137.    8.99    rh0    k1    k2
     0.0  1.4   0.727   0.0    eps5   gam5  cv5  b5
     8                         nrat
     0.000     0.2132            svt    aout
     3.810      .2132
     5.512      .1935
     7.112      .1427
     8.128      .0938
     8.687      .0446
     8.839      .0218
     8.890      .0218
     1.00e-04   1.00e-05      tinc   htop
     1.00e-05   1.00e-08      eps    srec
    22   0                    mf       kwrite
      60.0                    tmax
  rep1                        integrate once
  cham1                       compute p3
```

```
muzzle vel (m/sec)        776.0

max v pis  (m/sec)         23.4


max pl (mpa)              322.5

max p3 (mpa)              214.6

max p5 (mpa)             350.1

max pl (mpa)              201.7

max pr (mpa)              196.6


max acc (k-g)             19.8


max mass error            0.02

max energy error          0.08


ballistic efficiency =   15.27 %

expansion ratio =         3.41


loss to tube walls =      8.93 %


run time =     12.7     nstep =    3844
```

GLOSSARY

A_1 Area of the liquid reservoir, cm.^{2}

A_3 Area of the chamber, cm.^{2}

A_4 Area of the gun tube, cm.^{2}

A_e Area of the control rod at the transducer block, cm.^{2}

A_g Area of the grease dyke around the outer piston, cm.^{2}

A_h Area of the central hole in the outer piston, cm.^{2}

A_{h5} Area of the central hole in the block assembly, cm.^{2}

A_{mx} Maximum cross sectional area of the control rod, cm.^{2}

A_{rv} Area of the control rod at the reservoir vent, cm.^{2}

A_{r5} Area of the control rod (damper end), cm.^{2}

A_v Area of the reservoir injection vent, cm.^{2}

A_{v5} Area of the damper injection vent, cm.^{2}

A_{x5} Area of the control rod the damper pressure acts on, cm.^{2}

b Covolume, cm^3/g.

c_1 Speed of sound in the liquid in the reservoir, cm/s.

c_3 Speed of sound in the mixture in the chamber, cm/s.

c_4 Speed of sound in the mixture in the gun tube, cm/s.

c_5 Speed of sound in the damper fluid, cm/s.

C_D Discharge coefficient for the mass flux from the reservoir.

$C_D{'}$ Discharge coefficient for the mass flux into the gun tube.

e_1 Chemical energy of the liquid, j/g.

g_o Conversion constant = 10^7 g/MPa-cm-s.^{2}

h_{L1} Liquid enthalpy in the reservoir, j/g.

h_{G3} Gas enthalpy in the chamber, j/g.

h_{G4} Gas enthalpy in the gun tube, j/g.

m_{13} Mass flux from the reservoir into the chamber, g/s.

m_{34} Mass flux from the chamber into the gun tube, g/s.

M_4 Total mass in the gun tube, g.

m_{p3} Mass flux of the primer into the chamber, g/s.

m_5 Mass flux out of the damper, g/s.

M_{pu} Mass of the outer piston, g.

M_{pj} Mass of the projectile, g.

M_{rd} Mass of the control rod, g.

p_1 Pressure in the liquid reservoir, MPa.

p_3	Pressure in the combustion chamber, MPa.
p_5	Pressure in the damper, MPa.
p_{pa}	Piston resistance pressure, MPa.
p_R	Pressure at the base of the projectile, MPa.
p_t	Pressure at the gun tube entrance, MPa.
p_{pj}	Projectile resistance pressure, MPa.
Q_w	Heat loss to the gun tube walls, j/cm^3-s.
s_{pa}	Outer piston travel, cm.
s_{rd}	Control rod travel, cm.
s_{mv}	Difference in piston travels, cm.
t	Time, s.
V_1	Volume of the liquid reservoir, cm.^{3}
V_3	Volume of the combustion chamber, cm.^{3}
V_4	Volume of the gun tube behind the projectile, cm.^{3}
V_5	Volume of the damper, cm.^{3}
v_{pa}	Outer piston velocity, cm/s
v_{pj}	Velocity of the projectile, cm/s.
v_{rd}	Control rod velocity, cm/s.
v_{mv}	Difference in piston velocities, cm/s.
V_{mv}	Rate of change of the reservoir volume due to the relative motion of the pistons, cm^3/s.
v_t	Fluid velocity at the gun tube entrance, cm/s.
γ	Ratio of specific heats.
ρ_1	Liquid density in the reservoir, g/cm.^{3}
ρ_3	Mixture density in the chamber, g/cm.^{3}
ρ_4	Mixture density in the gun tube, g/cm.^{3}
ρ_5	Density of the damper fluid, g/cm.^{3}

2	Commander Naval Surface Warfare Center ATTN: O. Dengel K. Thorsted Silver Spring, MD 20902-5000
1	Commander Naval Surface Warfare Center ATTN: D.A. Wilson (Code G31) Dahlgren, VA 22448-5000
1	Commander Naval Surface Warfare Center ATTN: J. East (Code G33) Dahlgren, VA 22448-5000
1	Commander Naval Weapons Center China Lake, CA 93555-6001
1	AFOSR/NA (L. Caveny) Bldg. 410 Bolling AFB Washington, DC 20332
2	Director National Aeronautics and Space Administration ATTN: MS-603, Technical Library MS-86, Dr. Povinelli 21000 Brookpark Road Lewis Research Center Cleveland, OH 44135
1	Director Jet Propulsion Laboratory ATTN: Technical Library 4800 Oak Grove Drive Pasadena, CA 91109
3	Bell Aerospace Textron ATTN: F. Boorady F. Picirillo A.J. Friona P.O. Box One Buffalo, NY 14240
1	Calspan Corporation ATTN: Technical Library P.O. Box 400 Buffalo, NY 14225
1	General Electric Company Armament Systems Department ATTN: D. Maher Burlington, VT 05401

11	General Electric Ordnance Systems Division ATTN: J. Mandzy, OP43-220 R.E. Mayer H. West W. Pasko R. Pate J. Magoon J. Scudiere Minh Luu Lou Ann Walter Clare Cunningham R. DiNardi 100 Plastics Avenue Pittsfield, MA 01201-3698
1	IITRI ATTN: Library 10 W. 35th St. Chicago, IL 60616
1	Olin Chemicals Research ATTN: David Gavin P.O. Box 586 Chesire, CT 06410-0586
2	Olin Corporation ATTN: Victor A. Corso Dr. Ronald L. Dotson 24 Science Park New Haven, CT 06511
1	Safety Consulting Engr ATTN: Mr. C. James Dahn 5240 Pearl St. Rosemont, IL 60018
2	SAIC ATTN: Dr. F.T. Phillips Dr. Fred Su 10210 Campus Point Drive San Diego, CA 92121
1	SAIC ATTN: Norman Banks 4900 Waters Edge Drive Suite 255 Raleigh, NC 27606
1	Science Applications, Inc. ATTN: R. Edelman 23146 Cumorah Crest Woodland Hills, CA 91364
1	Sundstrand Aviation Operations ATTN: Mr. Owen Briles P.O. Box 7202 Rockford, IL 61125

No. of
Copies Organization

    1   Dr. Clive Woodley
         GS2 Division
         Building R31
         RARDE
         Ft. Halstead
         Sevenoaks, Kent TN14 7BT
         England

Intentionally left blank.

USER EVALUATION SHEET/CHANGE OF ADDRESS

This Laboratory undertakes a continuing effort to improve the quality of the reports it publishes. Your comments/answers to the items/questions below will aid us in our efforts.

1. BRL Report Number_____TR-3072_____Date of Report____DEC 89_____

2. Date Report Received_____

3. Does this report satisfy a need? (Comment on purpose, related project, or other area of interest for which the report will be used.)_____

_____

_____

4. How specifically, is the report being used? (Information source, design data, procedure, source of ideas, etc.)_____

_____

_____

5. Has the information in this report led to any quantitative savings as far as man-hours or dollars saved, operating costs avoided or efficiencies achieved, etc? If so, please elaborate._____

_____

_____

6. General Comments. What do you think should be changed to improve future reports? (Indicate changes to organization, technical content, format, etc.)

_____

_____

_____

	_____
	Name
CURRENT ADDRESS	_____
	Organization
	_____
	Address
	_____
	City, State, Zip

7. If indicating a Change of Address or Address Correction, please provide the New or Correct Address in Block 6 above and the Old or Incorrect address below.

	_____
	Name
OLD ADDRESS	_____
	Organization
	_____
	Address
	_____
	City, State, Zip

(Remove this sheet, fold as indicated, staple or tape closed, and mail.)

- - - - - - - - - - - FOLD HERE - - - - - - - - - - -

Director
U.S. Army Ballistic Research Laboratory
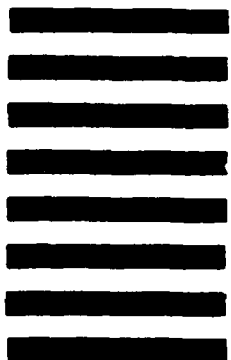ATTN: SLCBR-DD-T
Aberdeen Proving Ground, MD 21005-5066

OFFICIAL BUSINESS

BUSINESS REPLY MAIL
FIRST CLASS   PERMIT NO 12062   WASHINGTON, DC

POSTAGE WILL BE PAID BY DEPARTMENT OF THE ARMY

Director
U.S. Army Ballistic Research Laboratory
ATTN: SLCBR-DD-T
Aberdeen Proving Ground, MD 21005-9989

- - - - - - - - - - FOLD HERE - - - - - - - - - - -